Electron transport by the EXB-driven ion acoustic instability in a Hall thruster based on r-z multi-fluid simulations

— Part I —

I. Mikellides, A. Lopez Ortega, I. Katz
Jet Propulsion Laboratory, California Institute of Technology, Pasadena, CA

ExB Plasmas for Space and Industrial Applications Workshop, June 21 –23 2017, Toulouse, France.

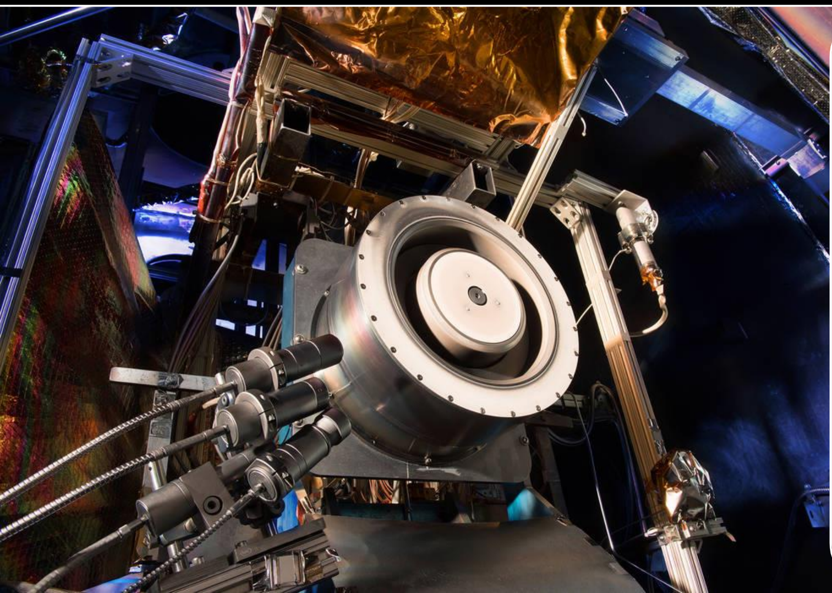

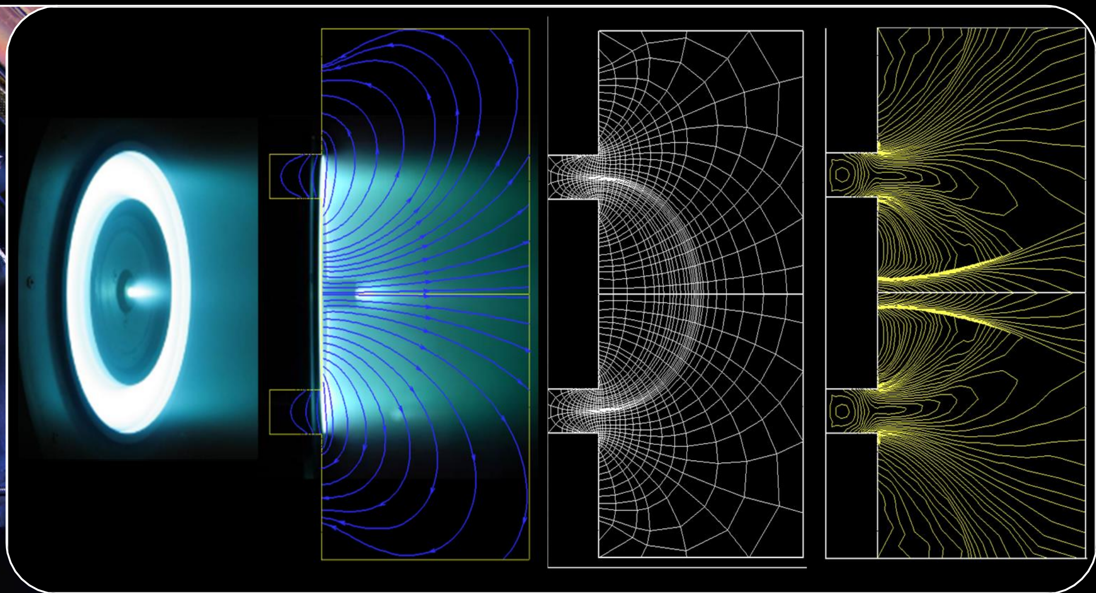

Modeling and Simulation of Electric Propulsion Plasmas Critical for NASA Science Missions

- The Hall-effect Rocket with Magnetic Shielding (HERMeS) is the first long-life Hall thruster developed for a NASA mission.
- HERMeS is designed to achieve service life of up to 50,000 h. ***Demonstration of such high throughputs requires a combination of wear tests and physics-based numerical simulation.***
- After the discovery of magnetic shielding, the physics behind anomalous transport remains the last long-standing problem in Hall thrusters.
  - Prohibits fully-predictive numerical simulations
  - Requires more testing and measurements to produce data required by numerical simulations
  - Increases thruster development time, cost and risk for the mission

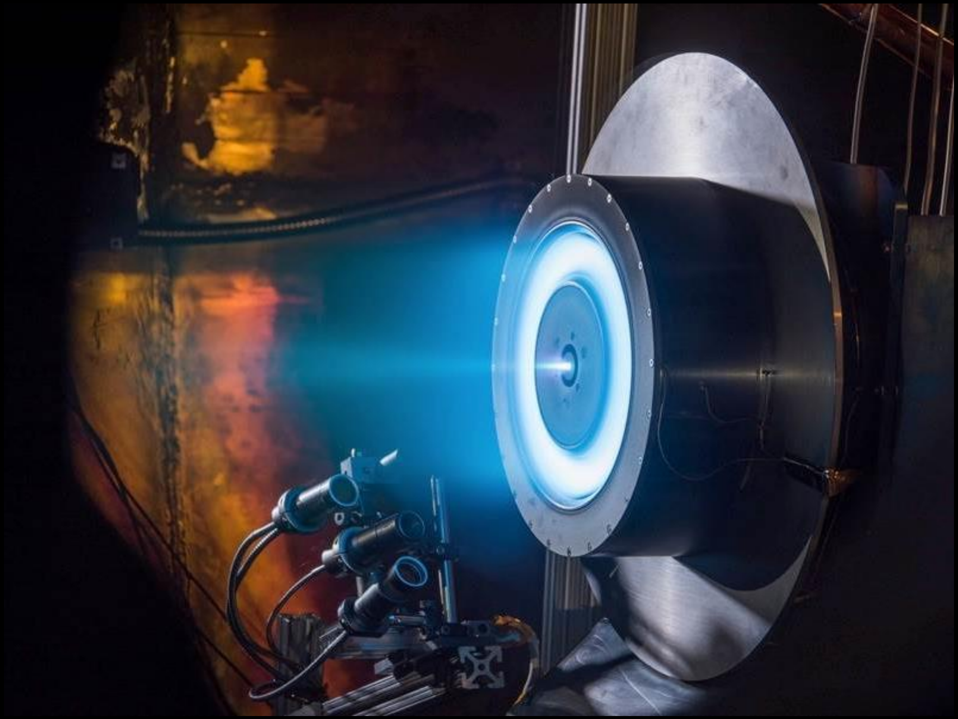

The **H**all-**E**ffect **R**ocket with **M**agn**e**tic **S**hielding (**HERMeS**) operating in VF-5 at the NASA Glenn Research Center

Predicting Channel and Pole Erosion in Hall Thrusters Requires at Least 2-D Axisymmetric Simulation in r-z Plane

- 1-D codes can provide insight into some fundamental aspects of Hall thruster operation fast, but are simply inadequate to provide the required level of detail.
- z-θ codes can provide critical insight into azimuthal physics but their ability to provide life-related assessments is limited.
- Steady-state/effective resistivity/marginal stability approaches offer better numerical stability but may fail to capture possibly inherent coupling between plasma dynamics.
- Computational resources for 3-D simulations remain too demanding.

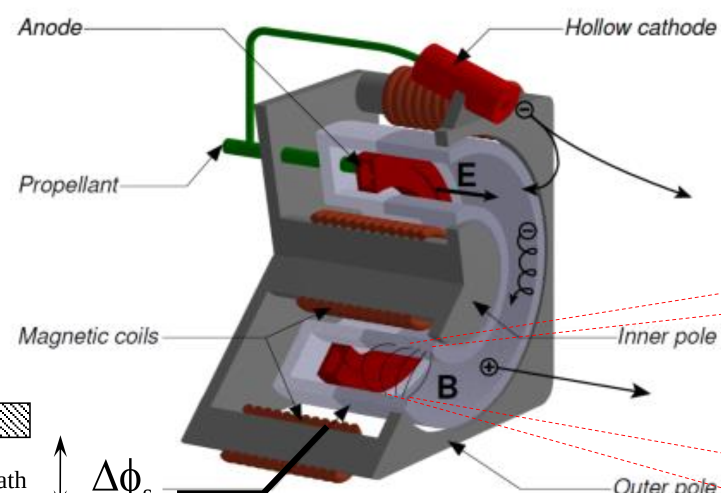

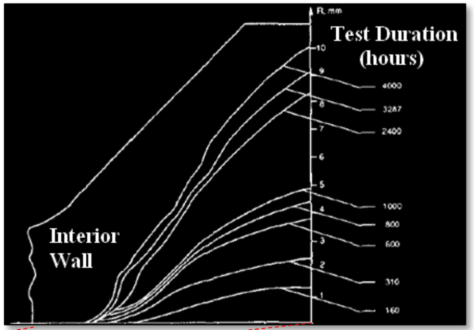

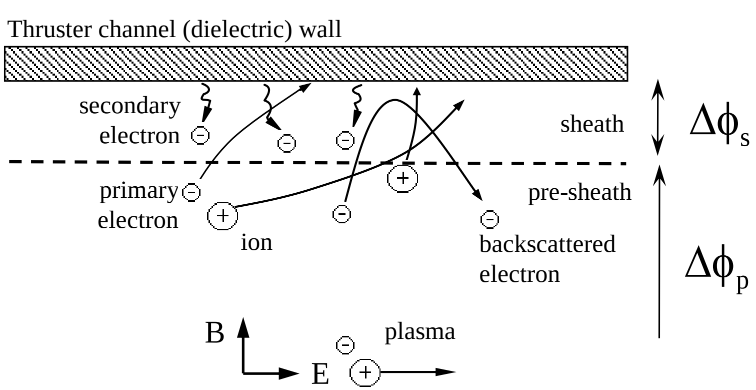

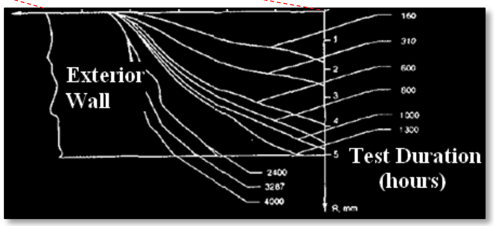

The 2-D Axisymmetric (r-z) Code Hall2De [1]

- Began development at JPL in 2008
- Discretization of all conservation laws on a magnetic field-aligned mesh
- Two components of the electron current density field accounted for in Ohm's law
- No statistical noise associated with the heavy-species conservation laws; Multiple ion fluid populations allowed
- Large computational domain, extending several times the thruster channel length

6 kW Lab Hall thruster

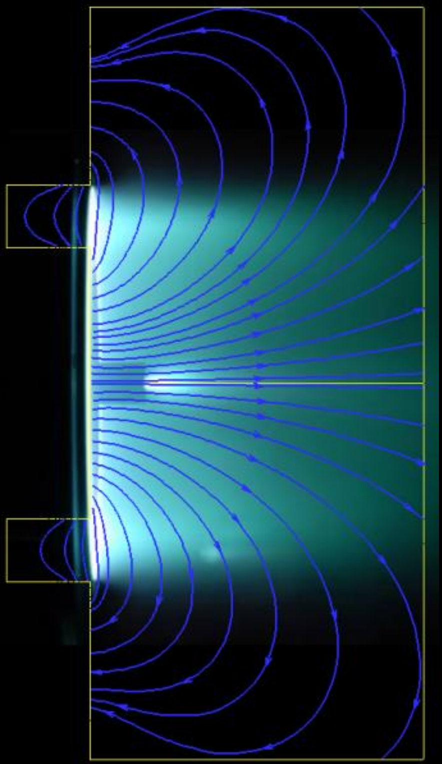

Magnetic field streamlines

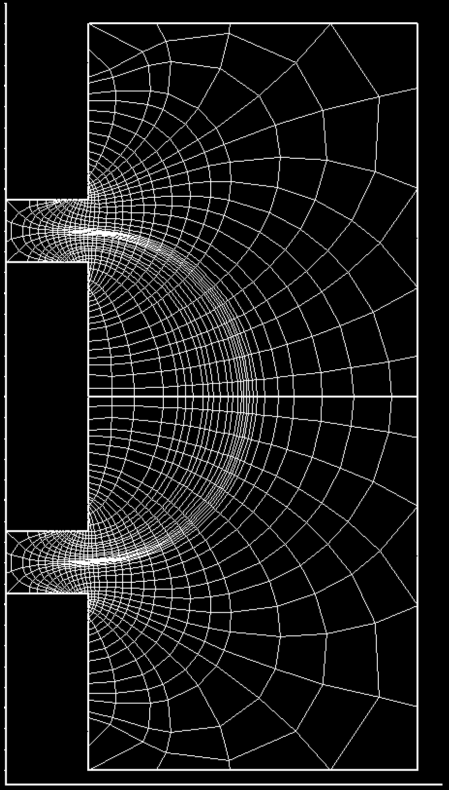

Hall2De computational mesh

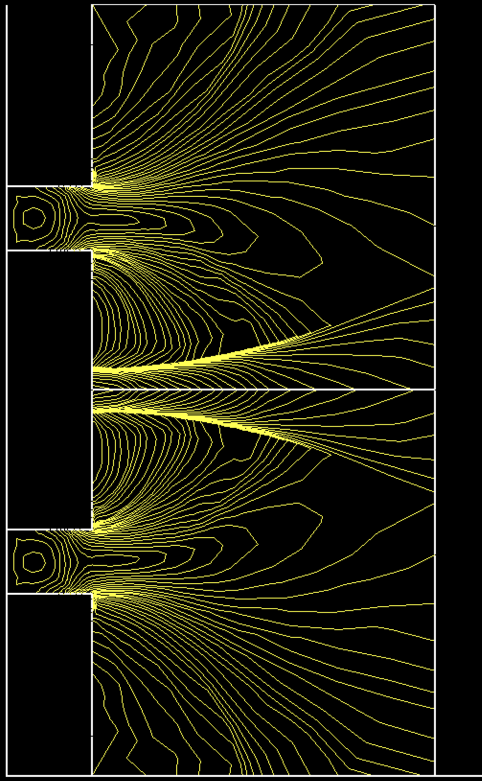

Ion density line contours

[1] Mikellides, I. G., and Katz, I., "Simulation of Hall-effect Plasma Accelerators on a Magnetic-field-aligned Mesh," Physical Review E, Vol. 86, No. 4, 2012, pp. 046703 (1-17).

Hall2De Equations for the Plasma

$$\frac{\partial n_i}{\partial t} + \nabla\cdot(n\mathbf{u})_i = \dot{n}, \qquad \dot{n} = \int \left(\dot{f}_i\right)_c d\mathbf{v}\Big|_{\text{inelastic}}$$

$$\frac{\partial}{\partial t}(nm\mathbf{u})_i + \nabla\cdot(nm\mathbf{u}\mathbf{u})_i = q_i n_i \mathbf{E} - \nabla p_i + \mathbf{R}_i$$

$$\mathbf{R}_i \approx -\sum_{s\neq i} n_i m_i \nu_{is}(\mathbf{u}_i - \mathbf{u}_s) + \int m_i \mathbf{v}\left(\dot{f}_i\right)_c d\mathbf{v}\Big|_{\text{inelastic}}$$

$$\nabla\cdot(\mathbf{j}_e + \mathbf{j}_i) = 0$$

$$\cancel{n_e m_e \frac{D\mathbf{u}_e}{Dt}} = -en_e(\mathbf{E} + \mathbf{u}_e \times \mathbf{B}) - \nabla p_e + \mathbf{R}_e$$

$$\rightarrow E_{//} = \eta j_{e//} - \frac{\nabla_{//} p_e}{en_e} + \eta_{ei}\bar{j}_{i//}, \quad E_{\perp} = \eta\left(1+\Omega_e^{\,2}\right) j_{e\perp} - \frac{\nabla_{\perp} p_e}{en_e} + \eta_{ei}\bar{j}_{i\perp}$$

$$\eta \equiv \frac{m_e(\nu_c + \nu_\alpha)}{e^2 n_e}$$

?

$$\frac{3}{2} en_e \frac{\partial T_e}{\partial t} = \mathbf{E}\cdot\mathbf{j}_e + \nabla\cdot\left(\frac{5}{2}T_e\mathbf{j}_e + \boldsymbol{\kappa}_e\cdot\nabla T_e\right) - \frac{3}{2}T_e\nabla\cdot\mathbf{j}_e - \sum_s \dot{n}e\left(\varepsilon + \frac{3}{2}T_e\right) + Q_e^T$$

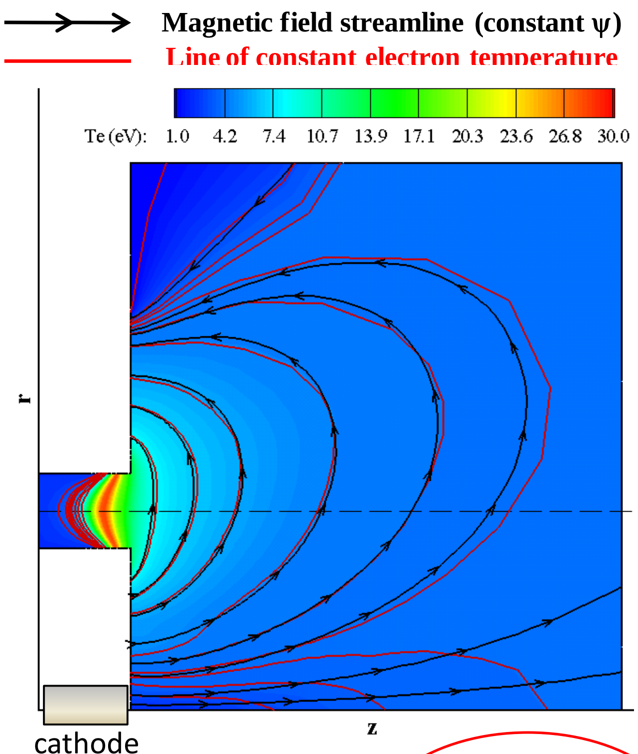

Extensive Effort Dedicated to Achieving a "Testbed" Plasma Solution that Can be used to Assess Anomalous Electron Transport Theories

- Several years of work have combined plasma measurements and r-z simulations with Hall2De to isolate the spatial variation of the anomalous collision frequency needed in Ohm's law.
- Hall2De plasma solution using empirically guided anomalous collision frequency now as close to a "measurement" as possible; can be used as a testbed.

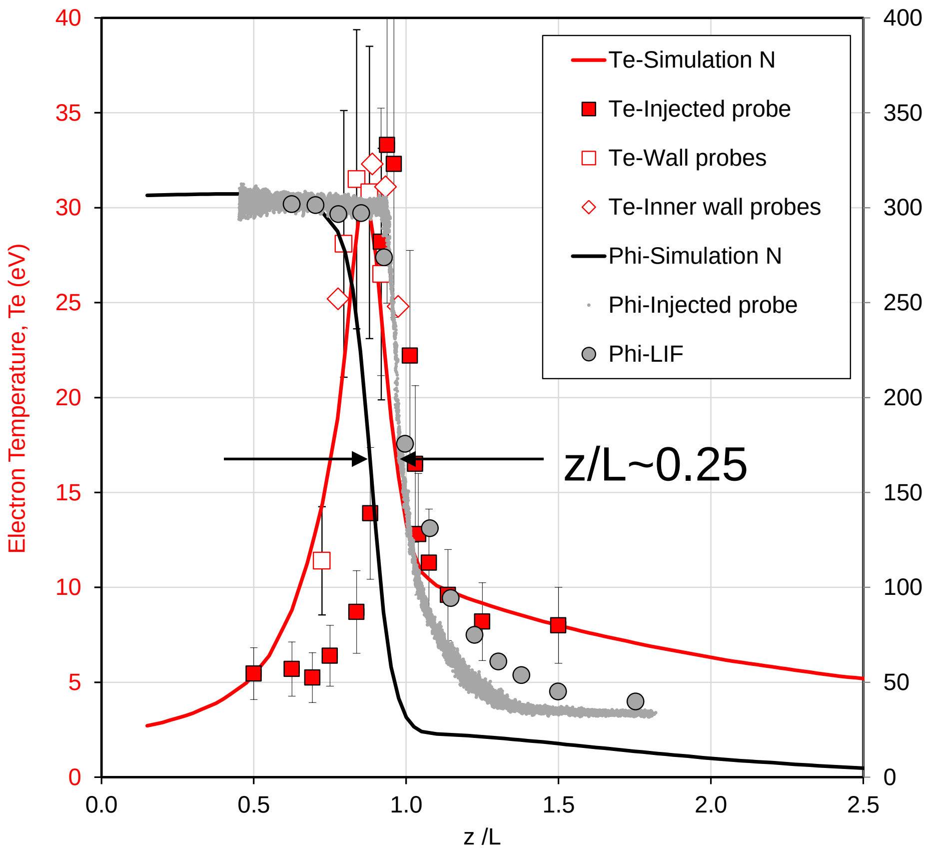

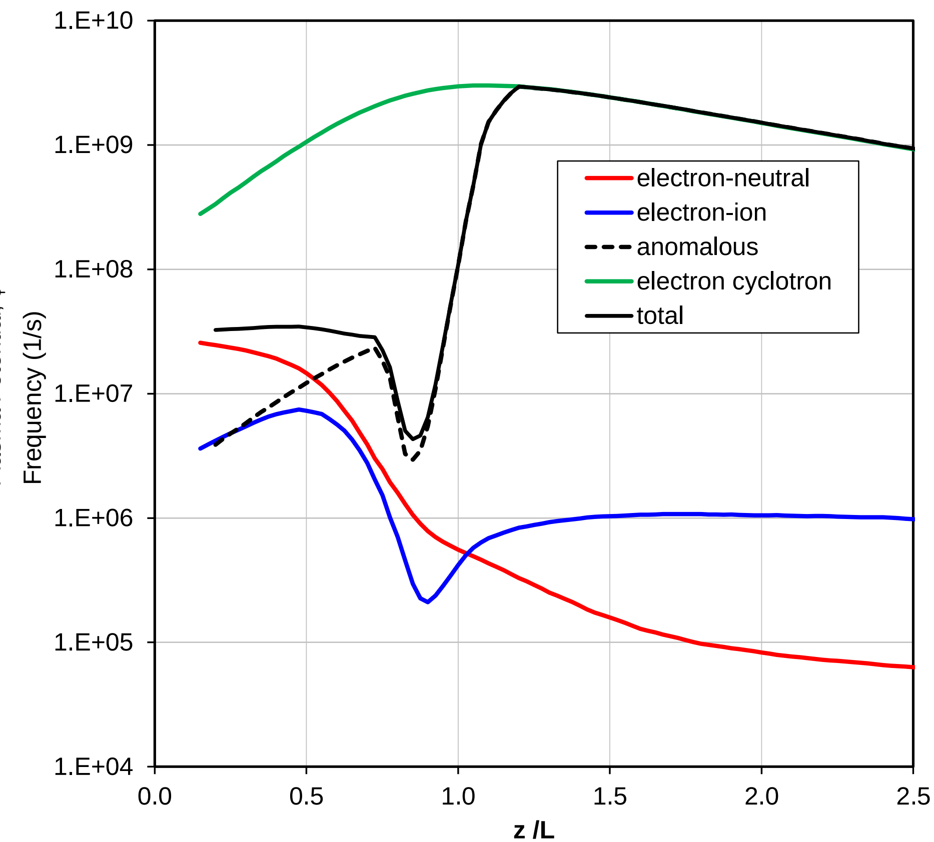

Uncertainties and Sensitivities Associated with the Hall2De "Testbed" Plasma Solution

- Required anomalous collision frequency deep in the channel interior difficult to quantify.

$$-\nabla_\perp \phi \approx \eta_\perp j_{e\perp} \sim \frac{B^2}{n_e \nu_e} j_{e\perp}$$

$$\mathbf{E}_\perp \cdot \mathbf{j}_{e\perp} \approx \eta_\perp j_{e\perp}^2 \sim \frac{B^2}{n_e \nu_e} j_{e\perp}^2$$

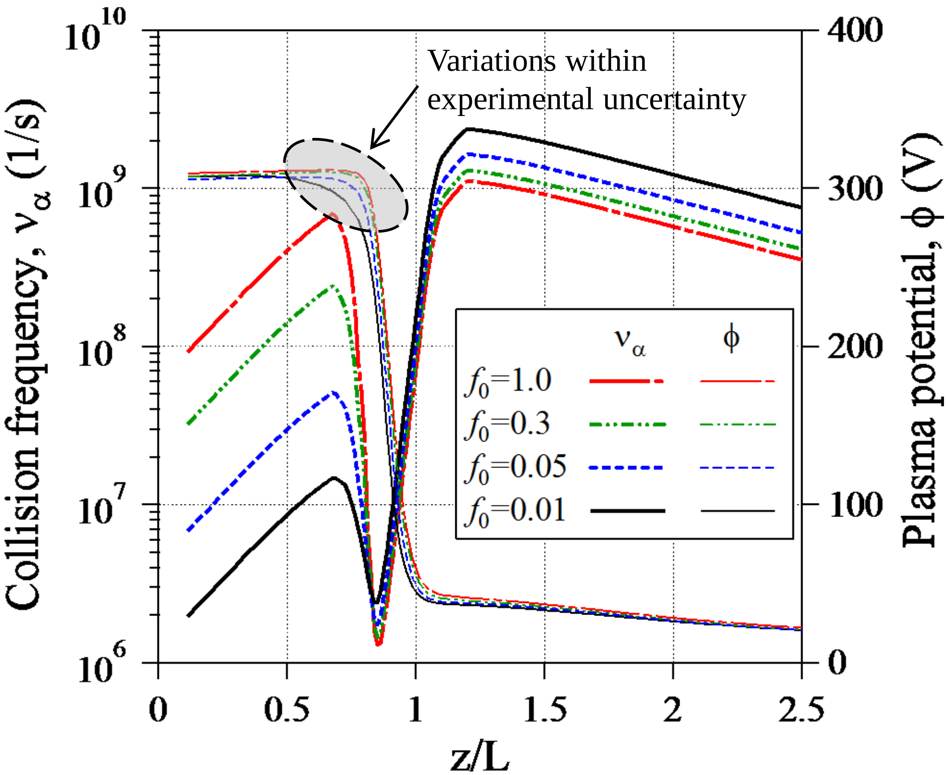

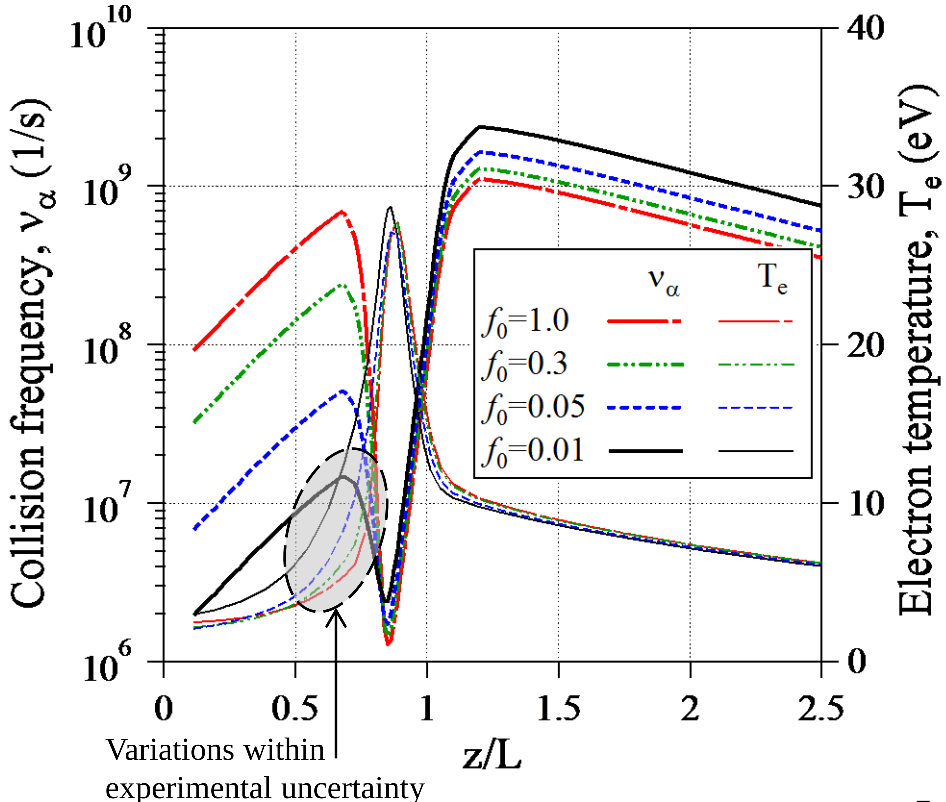

There Exists Strong Evidence Behind the Presence of **E×B**-driven Ion Acoustic Waves in Hall Thrusters

- Electron cyclotron drift waves identified in z-θ PIC simulations and proposed as source of anomalous electron tranposrt in Hall thrusters [1-4].
- Also in place is experimental evidence of high frequency micro-fluctuations in the **E×B** direction that exhibits linear dispersion [5].

PIC simulations in z-θ [4]

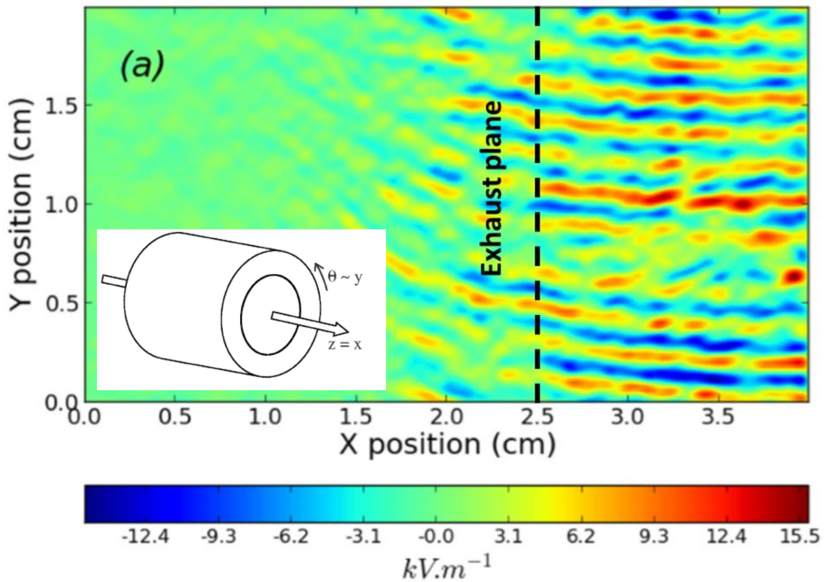

Dispersion measurements [5]

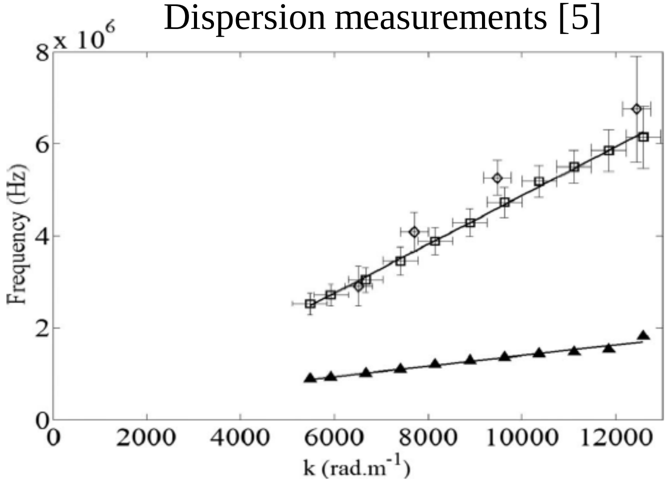

FIG. 5. Peak frequency variation with wave number, when $\vec{k}$ is oriented along $\vec{E}\times\vec{B}$. Open diamonds and open squares refer to two different experiments. The error bar length is a measure of the indetermination of the peak frequency. Full triangles are the root mean square of the best Gaussian fit to each peak. The peak frequency and the rms width are seen to increase linearly with the wave number.

[1] J. C. Adam, A. Héron, and G. Laval, "Study of stationary plasma thrusters using two-dimensional fully kinetic simulations", Physics of Plasmas 2004.
[2] A. Ducrocq, J. C. Adam, A. Héron, and G. Laval, "High-frequency electron drift instability in the cross-field configuration of Hall thrusters" Physics of Plasmas 2006
[3] A. Héron and J. C. Adam, "Anomalous conductivity in Hall thrusters: Effects of the non-linear coupling of the electron-cyclotron drift instability with secondary electron emission of the walls", Phys. Plasmas 2013
[4] P. Coche and L. Garrigues, "A two-dimensional (azimuthal-axial) particle-in-cell model of a Hall thruster", Physics of Plasmas 2014
[5] Tsikata, S., Lemoine, N., Pisarev, V., and Grésillon, D. M. Physics of Plasmas. Vol. 16., No. 3. 2009.

Testing the Theory that Anomalous Transport is Caused by the **E×B**-driven Ion Acoustic Instability

$$W = \frac{\varepsilon_0}{2}|\delta E|^2 \omega_r \frac{\partial \varepsilon}{\partial \omega}\Big|_{\omega=\omega_r} \qquad \varepsilon(\mathbf{k},\omega) = 1 + \sum_{j=e,i} \frac{\omega_{pj}}{k^2} \int \frac{\mathbf{k}\cdot\partial f_j/\partial \mathbf{v}}{\omega - \mathbf{k}\cdot\mathbf{v}}, \qquad \omega = \omega_r + i\gamma \qquad \omega_r = \mathbf{k}\cdot\mathbf{u}_i + \frac{kC_s}{\sqrt{1+k^2\lambda_D^2}}$$

$$\nu_\alpha \approx \omega_{pe}\frac{W}{en_eT_e} \quad \Longrightarrow \quad W_m \equiv \frac{\nu_\alpha}{\omega_{pe}} e n_e T_e$$

- **Wave energy density that is needed if ν_α~W**

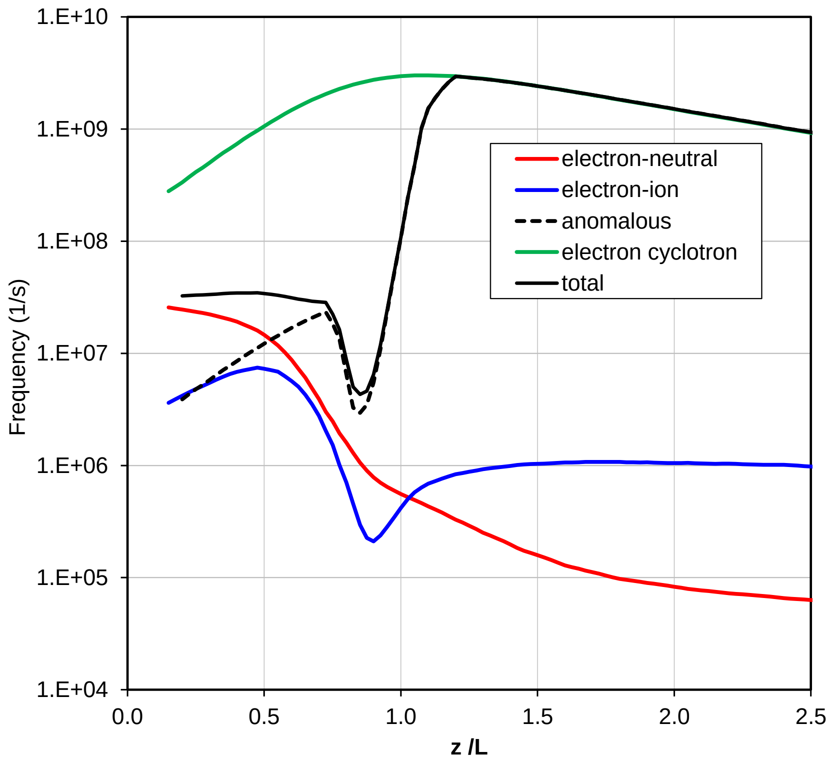

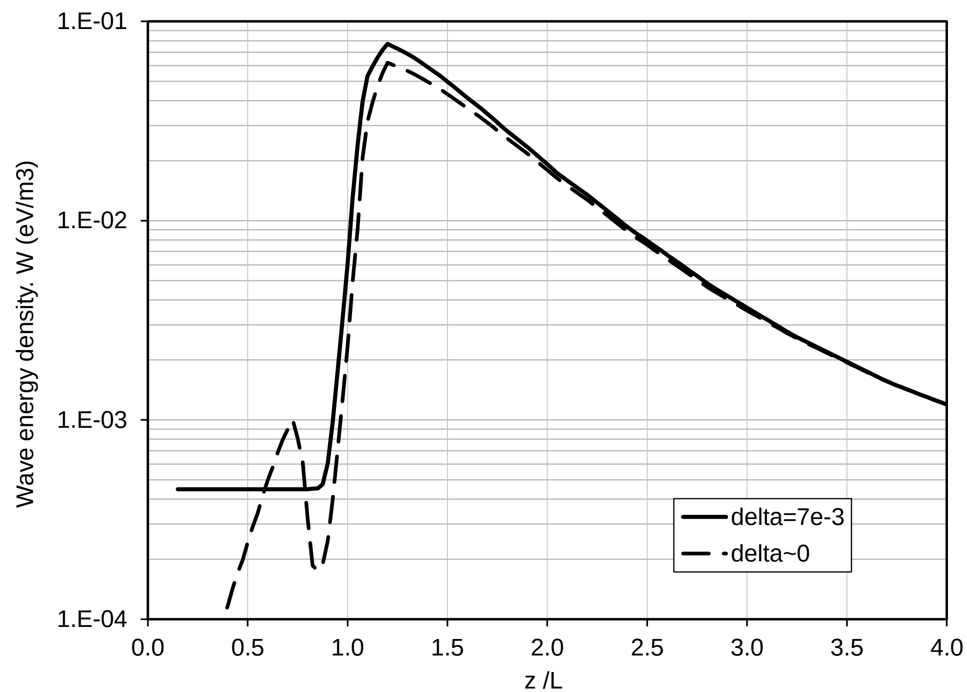

Testing the Theory that Anomalous Transport is Caused by the **E**×**B**-driven Ion Acoustic Instability

$$\frac{\partial W}{\partial t} + \nabla \cdot \left(W \mathbf{u}_i^+ \right) = 2\gamma W \qquad \gamma = \gamma_D - \left(\gamma_L + \nu_i \right)$$

• **Wave energy evolution equation.** Assumes wave energy generated from singly-charged ions comprising the main beam.

Testing the Theory that Anomalous Transport is Caused by the **E**×**B**-driven Ion Acoustic Instability

$$\frac{\partial W}{\partial t}+\nabla\cdot\left(W\mathbf{u}_i^{+}\right)=2\gamma W \qquad \gamma=\gamma_D-\left(\gamma_L+\nu_i\right)$$

• **Wave energy evolution equation.** Assumes wave energy generated from singly-charged ions comprising the main beam.

$$\boxed{\gamma_D=\gamma+\gamma_L+\nu_i}$$

Testing the Theory that Anomalous Transport is Caused by the **E**×**B**-driven Ion Acoustic Instability

$$\frac{\partial W}{\partial t} + \nabla \cdot \left(W \mathbf{u}_i^+\right) = 2\gamma W \xrightarrow{W=W_m} \gamma_m = \gamma_D - \left(\gamma_L + \nu_i\right)$$

• **Wave energy evolution equation.** Assumes wave energy generated from singly-charged ions comprising the main beam.

$$\boxed{\gamma_D = \gamma_m + \gamma_L + \nu_i}$$

• **Total growth rate**. In steady state the total growth rate must yield *this* value based on a combination of measurements and 2-D sims (testbed solution).

$$\gamma_m \equiv \frac{\nabla \cdot \left(W_m \mathbf{u}_i^+\right)}{2W_m}$$

Testing the Theory that Anomalous Transport is Caused by the **E**×**B**-driven Ion Acoustic Instability

$$\frac{\partial W}{\partial t}+\nabla\cdot\left(W\mathbf{u}_i^+\right)=2\gamma W \xrightarrow{W=W_m} \gamma_m=\gamma_D-\left(\gamma_L+\nu_i\right)$$

- **Wave energy evolution equation.** Assumes wave energy generated from singly-charged ions comprising the main beam.

$$\boxed{\gamma_D=\gamma_m+\gamma_L+\nu_i}$$

$$\nu_i=\sum_s \nu_{is}$$

- **Damping due to ion classical collisions**. All parameters to determine it known from combination of measurements and 2-D sims (testbed solution), except for ion temperature.

$$\gamma_L=\sqrt{\frac{\pi}{8}}\frac{\left|\omega_r\right|}{\left(1+k^2\lambda_D^2\right)^{3/2}}\left(\frac{T_e}{T_i}\right)^{3/2}\exp\left[-\frac{T_e}{2T_i\left(1+k^2\lambda_D^2\right)}\right]$$

- **Landau damping**. All parameters to determine it known from combination of measurements and 2-D sims (testbed solution), except for the ion temperature.

- **Total growth rate**. In steady state the total growth rate must yield *this* value based on a combination of measurements and 2-D sims (testbed solution).

$$\gamma_m\equiv\frac{\nabla\cdot\left(W_m\mathbf{u}_i^+\right)}{2W_m}$$

Testing the Theory that Anomalous Transport is Caused by the **E×B**-driven Ion Acoustic Instability

$$\frac{\partial W}{\partial t} + \nabla\cdot\left(W\mathbf{u}_i^+\right) = 2\gamma W \xrightarrow{W=W_m} \gamma_m = \gamma_D - \left(\gamma_L + \nu_i\right)$$

- **Wave energy evolution equation.** Assumes wave energy generated from singly-charged ions comprising the main beam.

$$\boxed{\gamma_D \overset{?}{=} \gamma_m + \gamma_L + \nu_i}$$

$$\nu_i = \sum_s \nu_{is}$$

- **Damping due to ion classical collisions**. All parameters to determine it known from combination of measurements and 2-D sims (testbed solution), except for ion temperature.

$$\gamma_D = \sqrt{\frac{\pi}{8}}\frac{|\omega_r|}{\left(1+k^2\lambda_D^2\right)^{3/2}}\left(\frac{E_\perp/B}{C_s}\sqrt{1+k^2\lambda_D^2}-1\right)\sqrt{\frac{m_e}{m_i}}$$

- **Destabilizing growth rate of ExB-driven ion acoustic waves**. All parameters to determine it known from combination of measurements and 2-D sims (testbed solution).

$$\gamma_L = \sqrt{\frac{\pi}{8}}\frac{|\omega_r|}{\left(1+k^2\lambda_D^2\right)^{3/2}}\left(\frac{T_e}{T_i}\right)^{3/2}\exp\left[-\frac{T_e}{2T_i\left(1+k^2\lambda_D^2\right)}\right]$$

- **Landau damping**. All parameters to determine it known from combination of measurements and 2-D sims (testbed solution), except for the ion temperature.

- **Total growth rate**. In steady state the total growth rate must yield *this* value based on a combination of measurements and 2-D sims (testbed solution).

$$\gamma_m \equiv \frac{\nabla\cdot\left(W_m\mathbf{u}_i^+\right)}{2W_m}$$

Comparisons Assuming Cold Ions ($T_i = T_n = 0.07$ eV)

$$\gamma_D \neq \gamma_m + \gamma_L + \nu_i$$

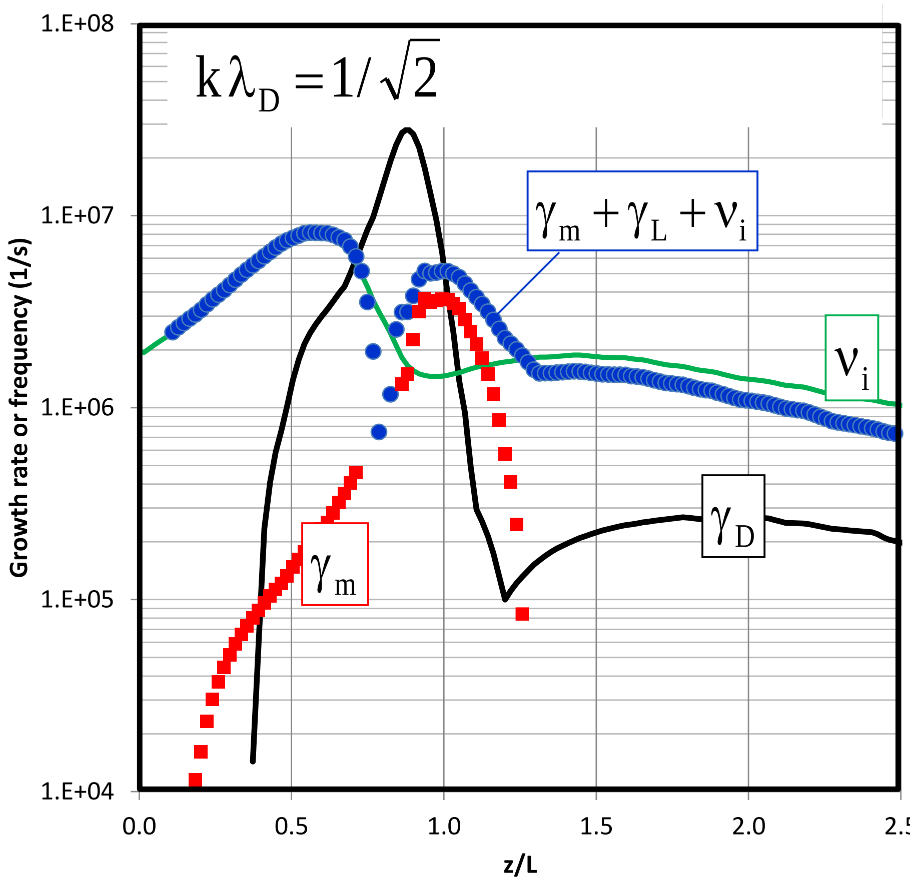

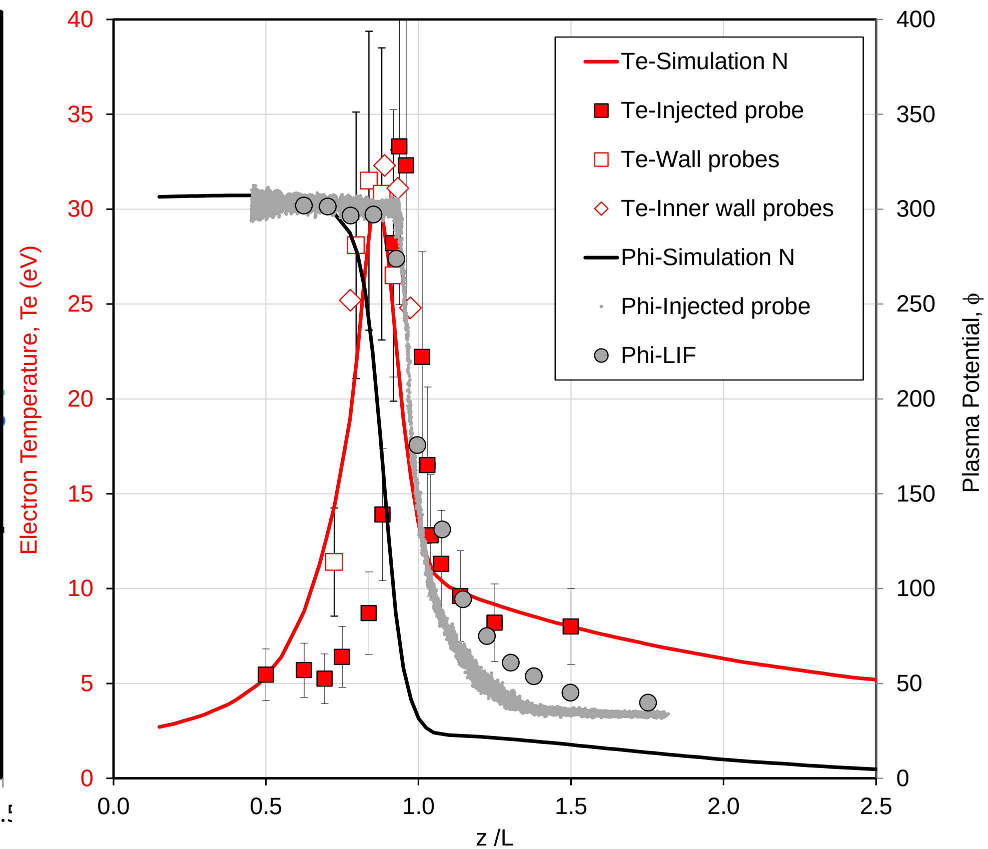

The Significance of the Ion Temperature

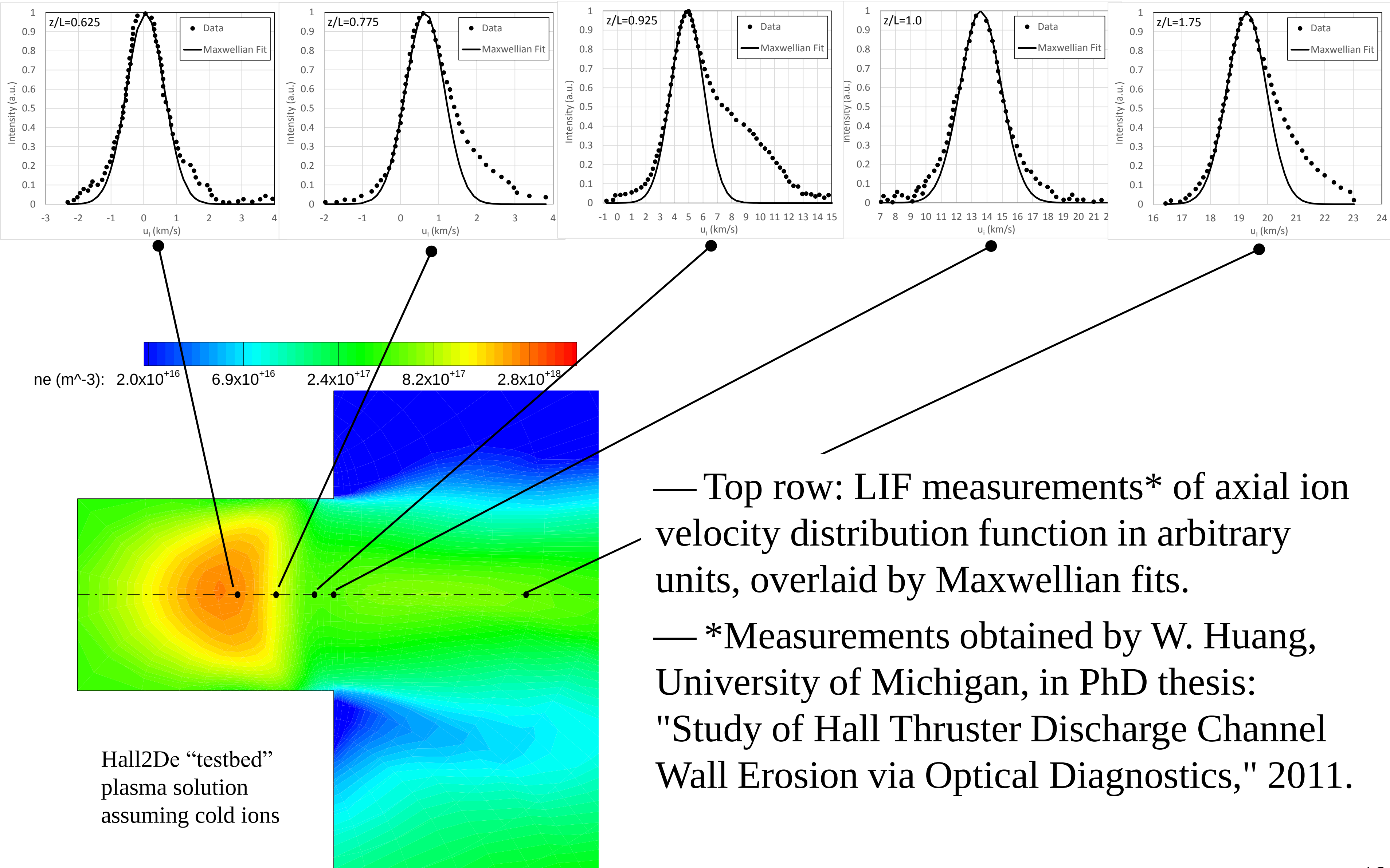

Hall2De "testbed" plasma solution assuming cold ions

- Top row: LIF measurements* of axial ion velocity distribution function in arbitrary units, overlaid by Maxwellian fits.
- *Measurements obtained by W. Huang, University of Michigan, in PhD thesis: "Study of Hall Thruster Discharge Channel Wall Erosion via Optical Diagnostics," 2011.

The Significance of the Ion Temperature

- Landau damping increases by many orders of magnitude if warm ions (based on LIF measurements) are taken into account compared to cold ions.

$$\gamma_L = \sqrt{\frac{\pi}{8}}\frac{|\omega_r|}{\left(1+k^2\lambda_D^2\right)^{3/2}}\left(\frac{T_e}{T_i}\right)^{3/2}\exp\left[-\frac{T_e}{2T_i\left(1+k^2\lambda_D^2\right)}\right]$$

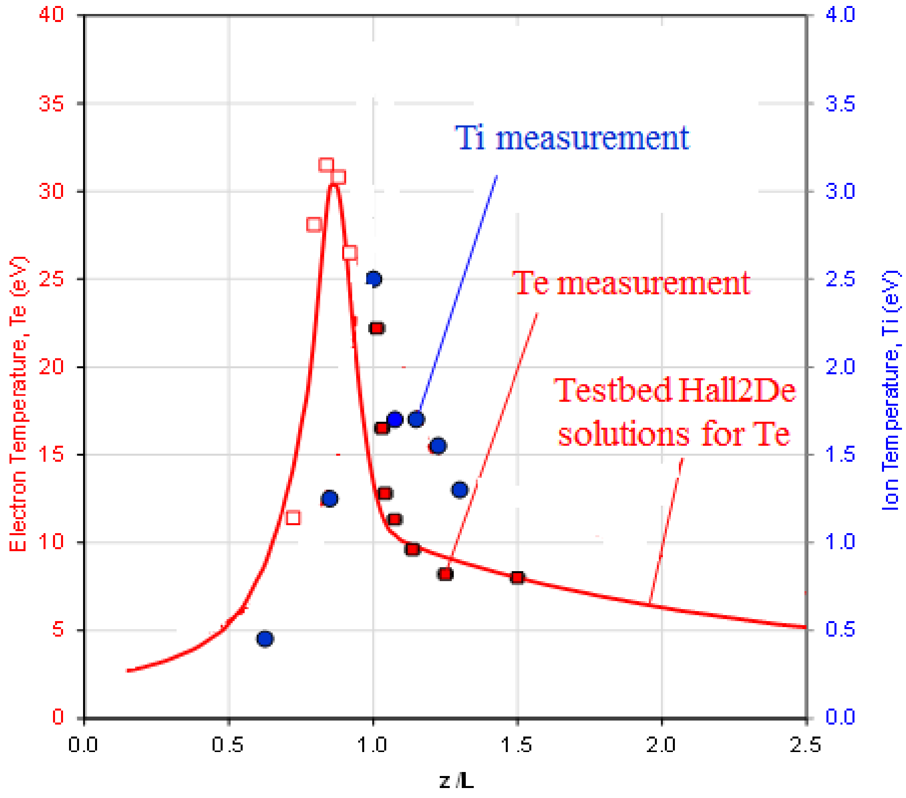

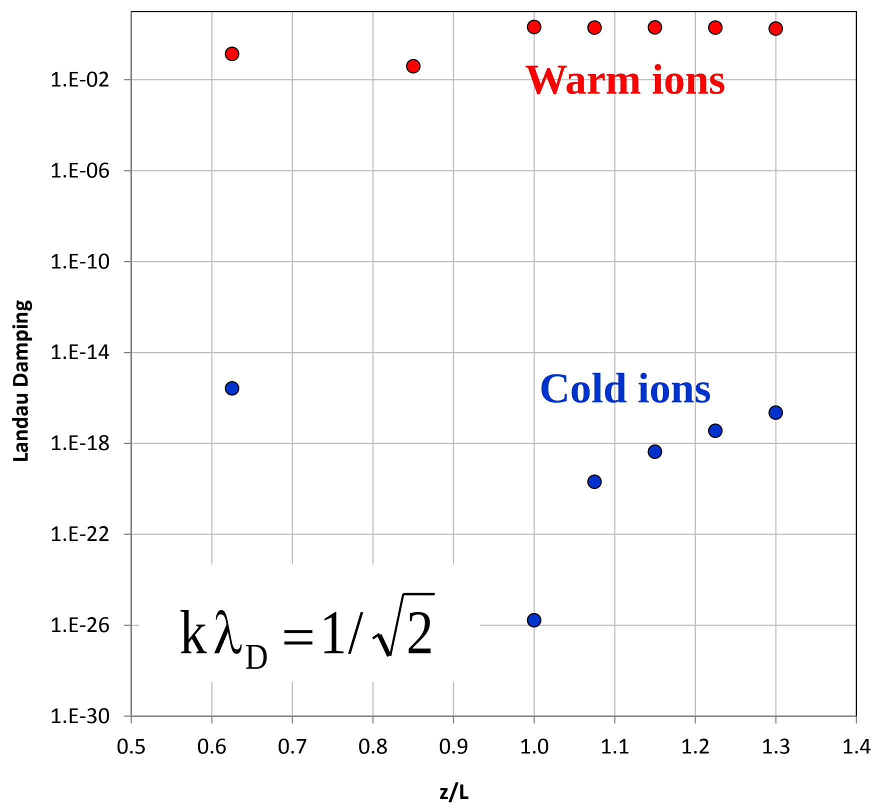

Growth Rate Comparisons After Accounting for Warm Ions

$$\gamma_D \approx \gamma_m + \gamma_L + \nu_i \qquad \gamma_D \neq \gamma_m + \gamma_L + \nu_i$$

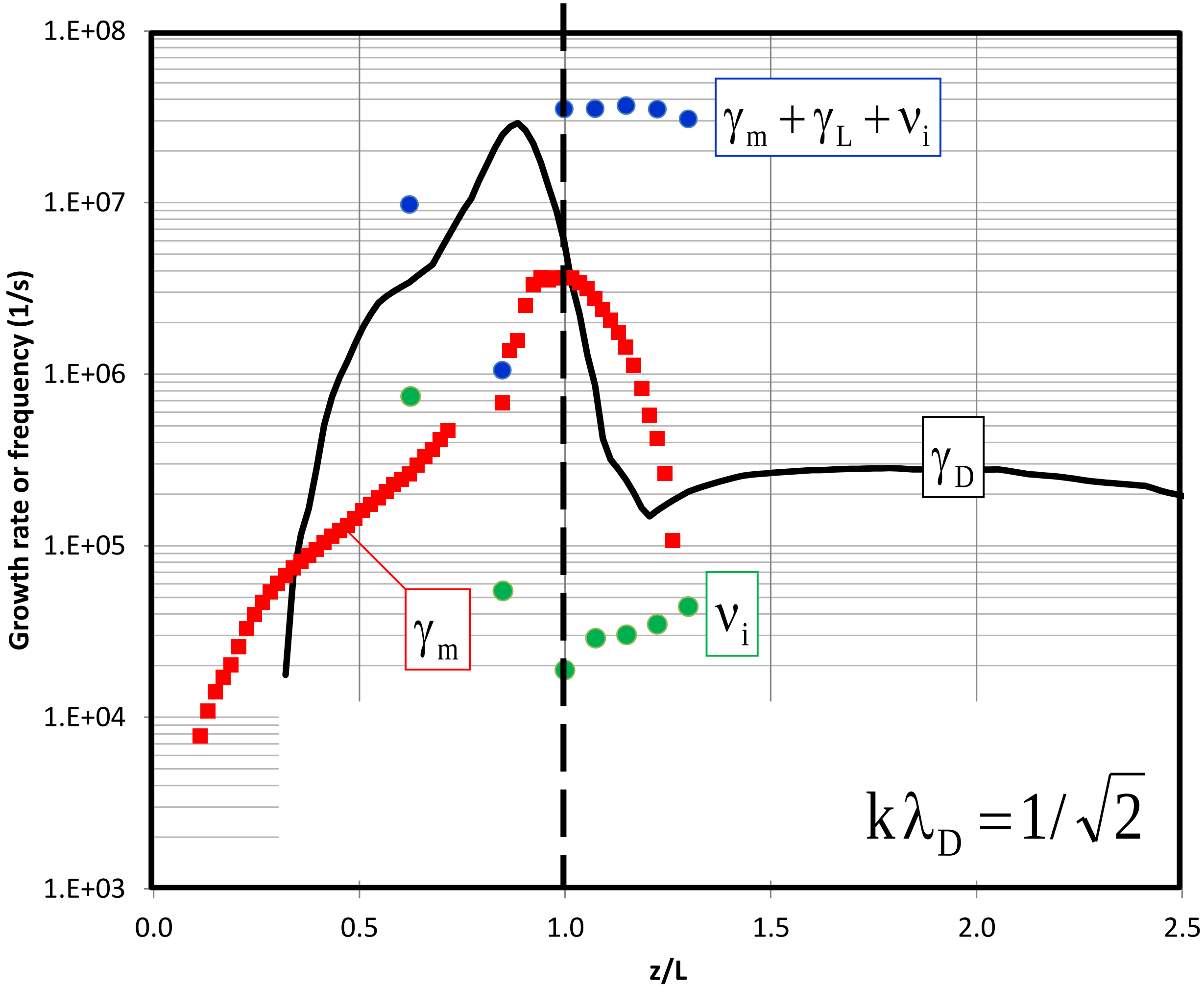

- Destabilization of **E×B-**driven ion acoustic waves associated with Xe^+ beam ions possible in the channel interior, but <u>not</u> in the near plume where the waves are severely (Landau) damped.
- Convection of waves to the plume <u>not</u> sufficient to achieve the energy density needed there.

Electron transport by the EXB-driven ion acoustic instability in a Hall thruster based on r-z multi-fluid simulations

— Part II —

A. Lopez Ortega, I. Katz, V. Chaplin, I. Mikellides
Jet Propulsion Laboratory, California Institute of Technology, Pasadena, CA

ExB Plasmas for Space and Industrial Applications Workshop, June 21 –23 2017, Toulouse, France.

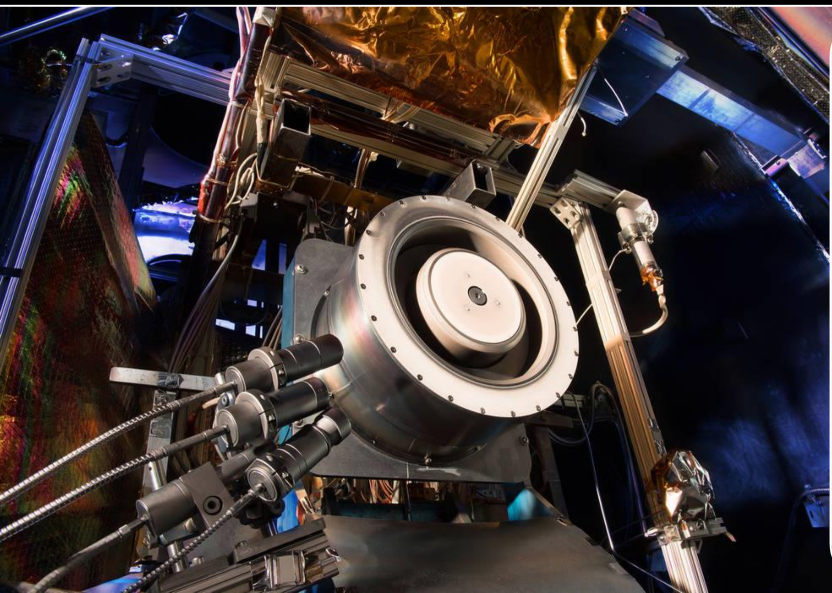

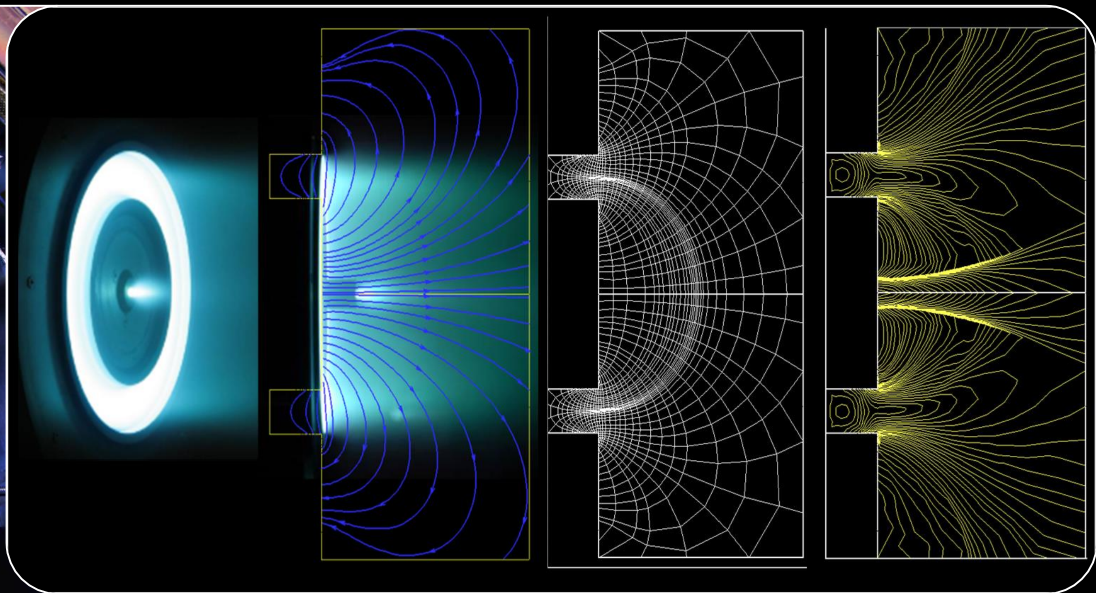

Theoretical growth of instability in acceleration region is higher than the “needed” growth

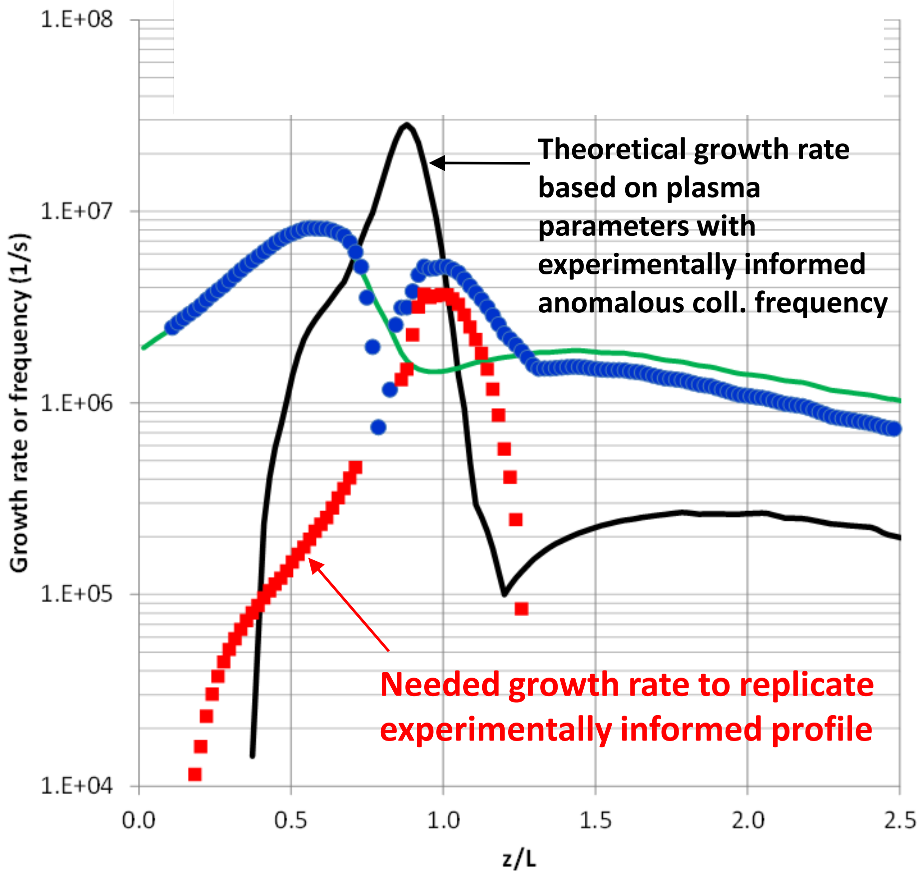

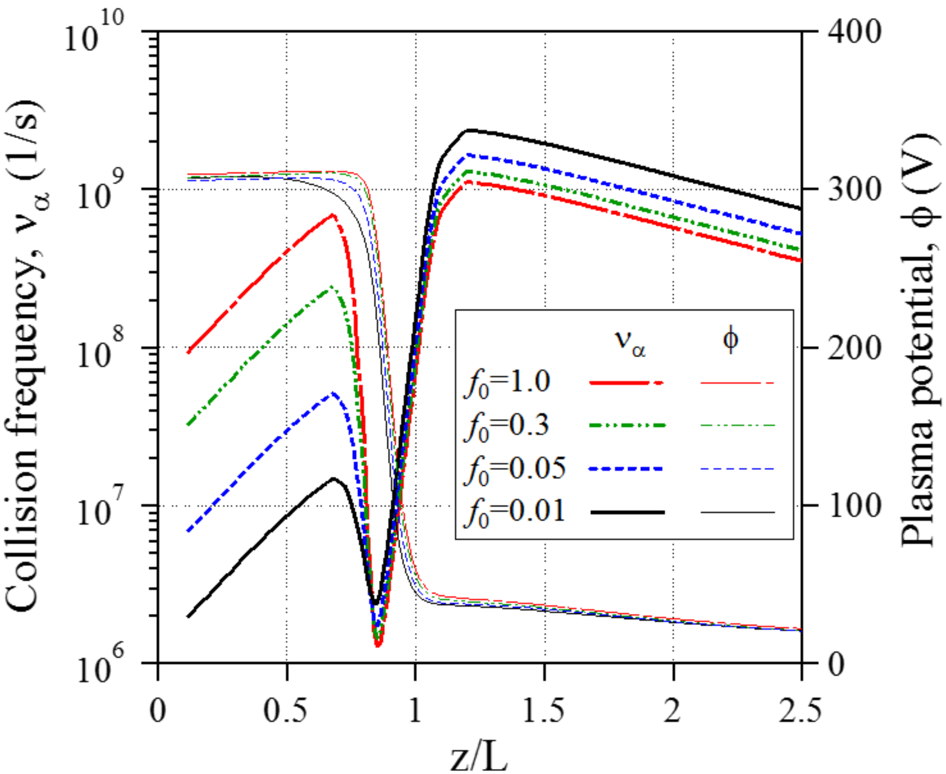

- The anomalous collision frequency is found to have a minimum at the acceleration region. However, the theoretical growth rate predicted by such plasma potential profile is conductive to large growth rates of the instability, which in turn should result in large values of the wave energy density and the anomalous collision frequency.
- Our efforts have been focused on eliminating the growth in the acceleration region by means of, for instance, Landau damping. All our efforts have been unsuccessful as even significant Landau damping cannot completely counteract the maximum growth rate.

Can accounting for multiple wave-lengths improve our self-consistent model?

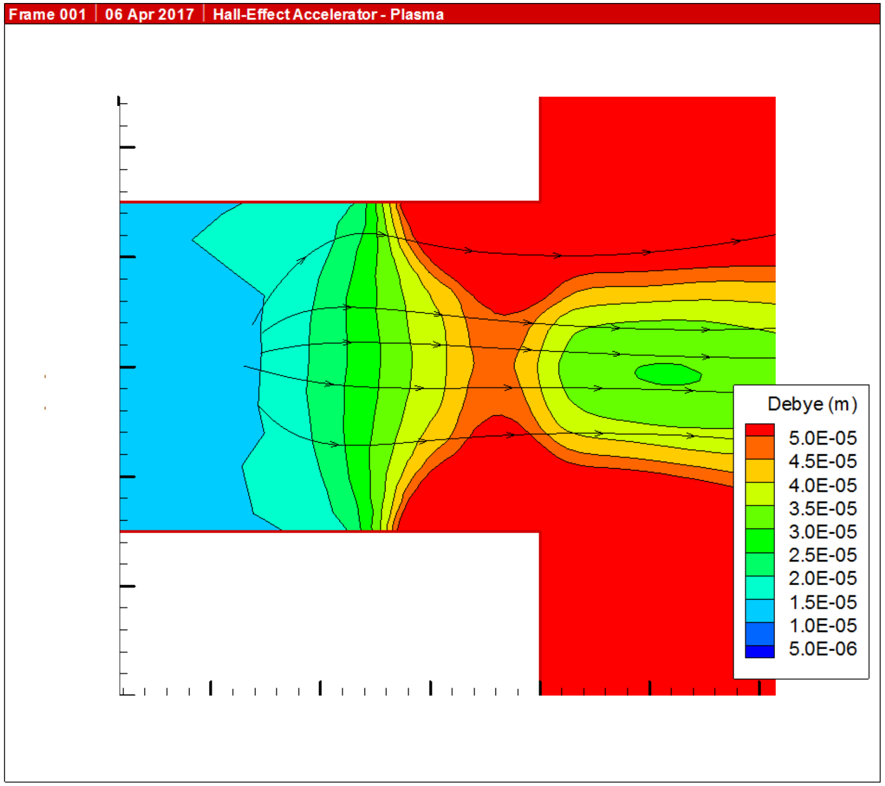

- For the H6, the Debye length increases by a factor of 5, following ion streamlines.
- Neglecting Landau damping, the maximum growth occurs for $k = 1/\sqrt{2\lambda_{De}^2}$. Waves of wavelength that have maximum growth inside the channel may be damped as the Debye length increases, while other waves with lower k may start growing further downstream.
- Addition of Landau damping may change the wave-length of maximum growth at a given location.
- **Proposed algorithm**: solve a discrete number of equations for the wave actions associated with multiple wavelengths. The total anomalous collision frequency can be obtained as the sum of all contributions.

Summary of equations for discrete wave-length model for wave action

$$\boxed{\frac{\partial N_k}{\partial t}+\nabla\cdot\left(\left(\nabla_k\omega_{r,k}\right)N_k\right)-\nabla_k\cdot\left(\left(\nabla\omega_{r,k}\right)N_k\right)=2\omega_{i,k}N_k}$$

$$c_s=\sqrt{qT_e/m_i} \qquad v_{te}=\sqrt{qT_e/m_e}$$

$$\omega_{r,k}=\mathbf{u}_i\cdot\mathbf{k}+c_s\frac{k}{\left(1+k^2\lambda_{De}^2\right)^{1/2}}$$

$$\omega_{i,k}=\left(\frac{\pi}{8}\right)^{1/2}\frac{c_s k}{\left(1+k^2\lambda_{De}^2\right)^{3/2}}\left(\frac{\mathbf{k}\cdot\mathbf{u}_{ei}-kc_s/\left(1+k^2\lambda_{De}^2\right)^{1/2}}{kv_{te}}\exp\left(-\frac{1}{2}\left(\frac{\mathbf{k}\cdot\mathbf{u}_{ei}-kc_s/\left(1+k^2\lambda_{De}^2\right)^{1/2}}{kv_{te}}\right)^2\right)-\sum_i\frac{n_i}{n_e}\frac{T_e^{3/2}}{T_i^{3/2}\left(1+k^2\lambda_{De}^2\right)^{1/2}}\exp\left(-\frac{T_e}{2T_i\left(1+k^2\lambda_{De}^2\right)}\right)\right)-\frac{1}{2}\nu_i$$

$$\boxed{\nu_{an}=\left(\frac{\pi}{2}\right)^{1/2}\sum_k\frac{qk^2N_k}{n_e\sqrt{m_e m_i}\left(1+k^2\lambda_{De}^2\right)^{3/2}}\exp\left(-\left(\frac{\hat{k}\cdot\mathbf{u}_{ei}-c_s/\left(1+k^2\lambda_{De}^2\right)^{1/2}}{v_{te}}\right)^2\right)}$$

We also accounted in our model for anomalous heating of ions:

$$\frac{3}{2}n_i\frac{\partial T_i}{\partial t}+n_i\nabla\cdot\left(\mathbf{u}_iT_i\right)+\frac{n_i\mathbf{u}_i}{2}\cdot\nabla T_i=Q_i+\dot{n}_i\left(\varepsilon_i-\frac{3}{2}T_i\right)+Q_{an(i)}$$

$$Q_{an(i)}=\frac{qn_i}{n_e}\sum_k N_k c_s k\left(\frac{\sqrt{\pi/2}\,\omega_{r,k}}{\left(1+k^2\lambda_{De}^2\right)^{3/2}}\left(\frac{\mathbf{k}\cdot\mathbf{u}_{ei}-kc_s/\left(1+k^2\lambda_{De}^2\right)^{1/2}}{kv_{te}}\exp\left(-\frac{1}{2}\left(\frac{\mathbf{k}\cdot\mathbf{u}_{ei}-kc_s/\left(1+k^2\lambda_{De}^2\right)^{1/2}}{kv_{te}}\right)^2\right)\right)-\frac{\omega_{i,k}}{\left(1+k^2\lambda_{De}^2\right)^{1/2}}\right)$$

Wave action distribution along centerline based on experimentally informed solution background plasma

- First check for self-consistent model: **experimentally informed solution** as background for computing anomalous collision frequency based on the previous equations. **Then compare result with the experimentally informed collision frequency.**
- **Ion temperature is computed including anomalous heating**. This has negligible effect of momentum $(nE \gg \nabla(nT))$ but affects growth rate $\omega_{i,k}$.

Some wavelengths exhibit growth inside channel

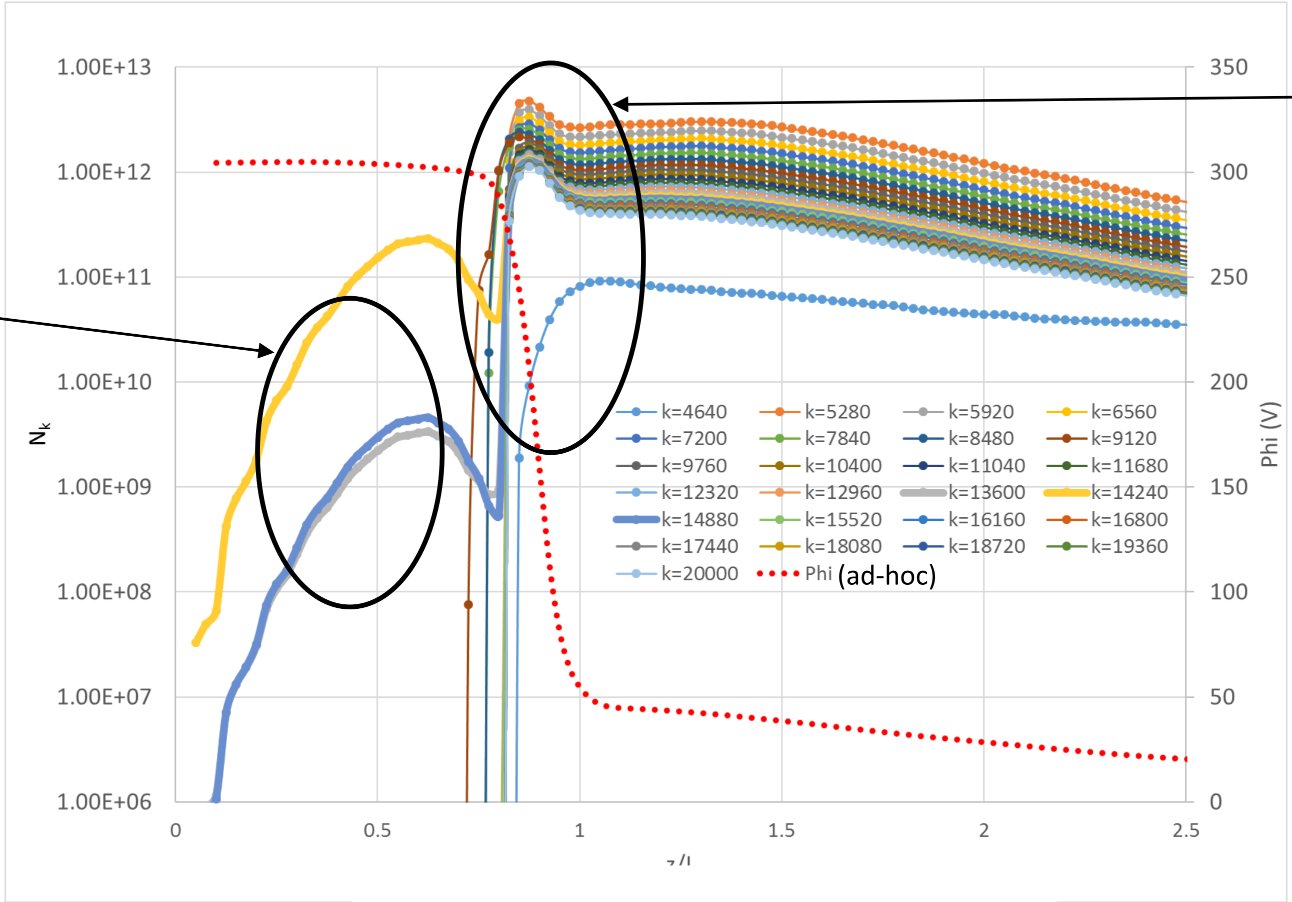

Growth of wave action in region of large electric fields for all wavelengths

Multiple wave-length model do not produce results that agree with measurements

- First check for self-consistent model: **experimentally informed solution** as background for computing anomalous collision frequency based on the previous equations. **Then compare result with the experimentally informed collision frequency.**
- **Ion temperature is computed including anomalous heating**. This has negligible effect of momentum ($nE \gg \nabla(nT)$) but affects growth rate $\omega_{i,k}$.

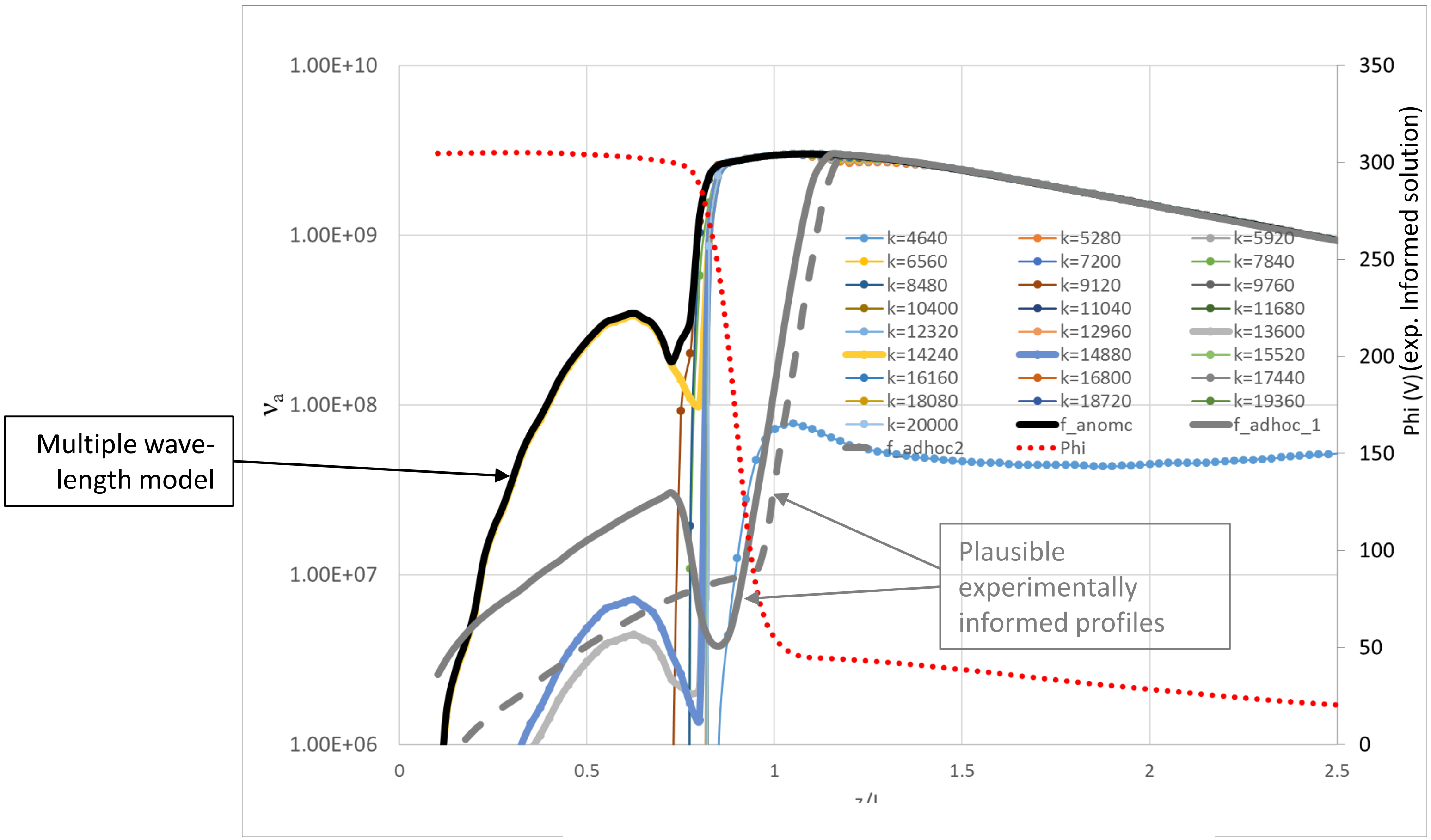

Multiple wave-length model do not produce results that agree with measurements

- Results of the first test suggest that a **fully self-consistent simulation** will produce results that are very different to those of the experimentally informed solution.

Very flat plasma potential

Due to small electric field, only two wavelengths exhibit growth

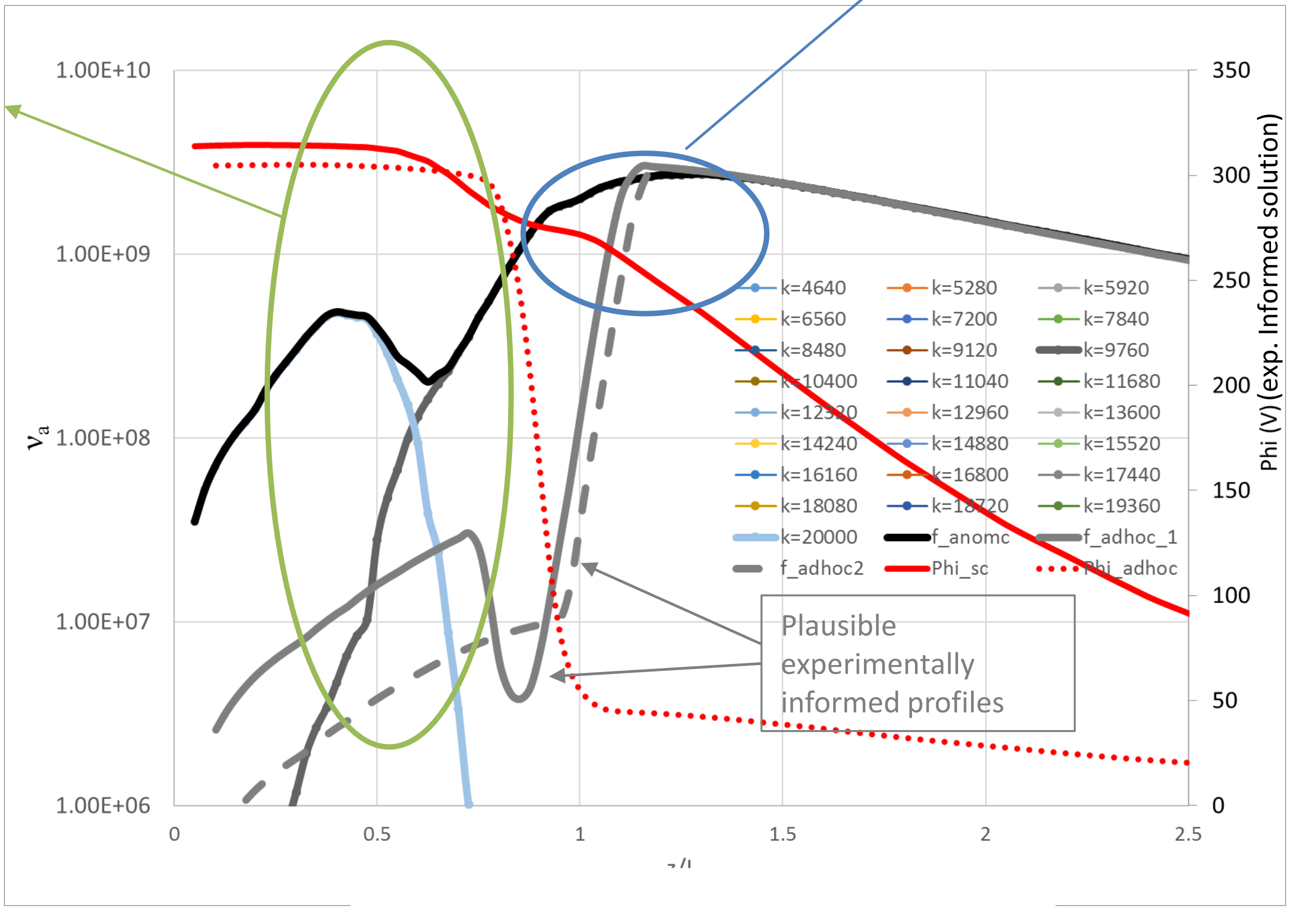

Total resistivity in the plasma is low, discharge current 57 A vs 20 A of experimentally informed solution

Accepting that there is going to be growth of the instability in the acceleration region

- So far, we relied on trying to decrease the growth rate of the instability in the acceleration region by means of a damping mechanism, such as Landau damping.

- Follow a new approach: what if growth of the instability still occurs, but the electrons do not interact with the waves at certain locations?

- **One basic idea is to compare the energy associated with the ion drift with the energy of the wave perturbations**

$$\phi_{drift} \approx \frac{m_e |\mathbf{E}|^2}{2q|\mathbf{B}|^2} \qquad \phi_k = \sqrt{\frac{kT_e^2 N_k}{n_e m_i \left(1+k^2\lambda_{De}^2\right)^{3/2}}}$$

- We compute an auxiliary variable ξ by means of a heat equation

$$\frac{\partial \xi_k}{\partial t} - K_1 \nabla^2 \xi_k = \frac{\phi_{drift}}{\phi_k}$$

- And assume that when ξ is large, the anomalous collision frequency is not affected by the wave action

$$\nu_{an} = \left(\frac{\pi}{2}\right)^{1/2} \sum_k \boxed{f_k} \frac{qk^2 N_k}{n_e \sqrt{m_e m_i}\left(1+k^2\lambda_{De}^2\right)^{3/2}} \exp\left(-\left(\frac{\hat{k}\cdot\mathbf{u}_{ei} - c_s \big/ \left(1+k^2\lambda_{De}^2\right)^{1/2}}{v_{te}}\right)^2\right)$$

$$f_k = \exp\left(-K_2 \xi_k\right)$$

Setting a limit to the drift velocity

- Simulations showed that the anomalous collision frequency can become almost zero with this model as a consequence of the plasma potential gradient becoming very steep.

- To avoid this circumstance, we also included a simple model for computing the floor value of the anomalous collision frequency.

- The model relies on the fact that the Mach number for electrons cannot exceed 1, as other instabilities characterized by shorter time-scales (i.e., two-stream instability for electrons) may occur.

$$\sqrt{\frac{qT_e}{m_e}} \geq \frac{j_{e\wedge}}{qn_e} = \Omega_e \frac{j_{e\perp}}{qn_e} = \frac{qB}{m_e\left(\nu_{ei}+\nu_{en}+\nu_a\right)}\frac{j_{e\perp}}{qn_e}$$

$$\nu_{a,floor} = \frac{B}{m_e n_e}\frac{j_{e\perp}}{\sqrt{qT_e/m_e}} - \nu_{ei} - \nu_{en}$$

Wave action distribution along centerline with new model is unmodified (as expected)

- First check for self-consistent model: **experimentally informed solution** as background for computing anomalous collision frequency based on the previous equations. **Then compare result with the experimentally informed collision frequency.**

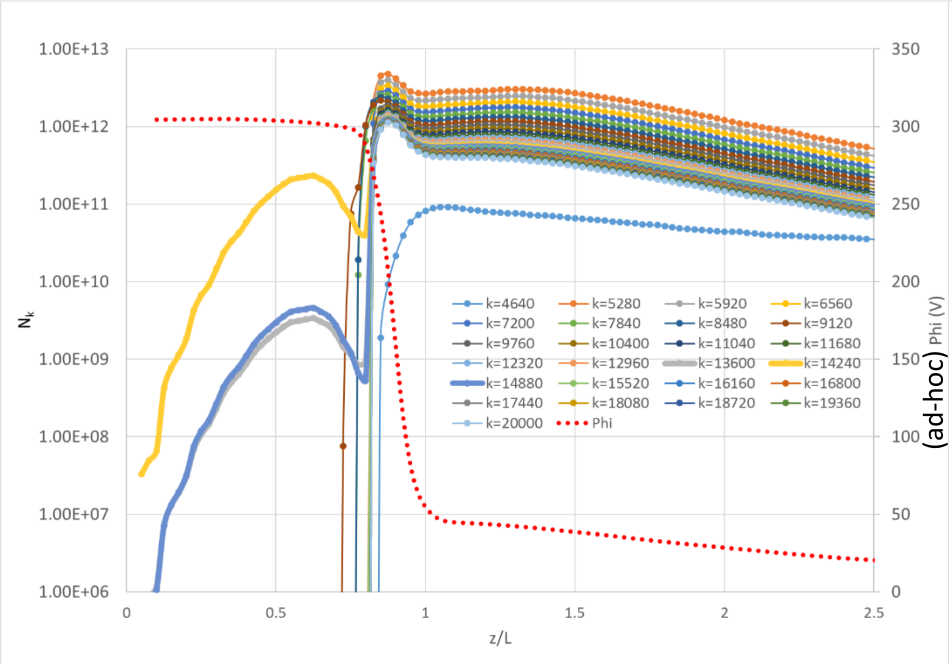

Model with correction factor f_k in anomalous collision frequency

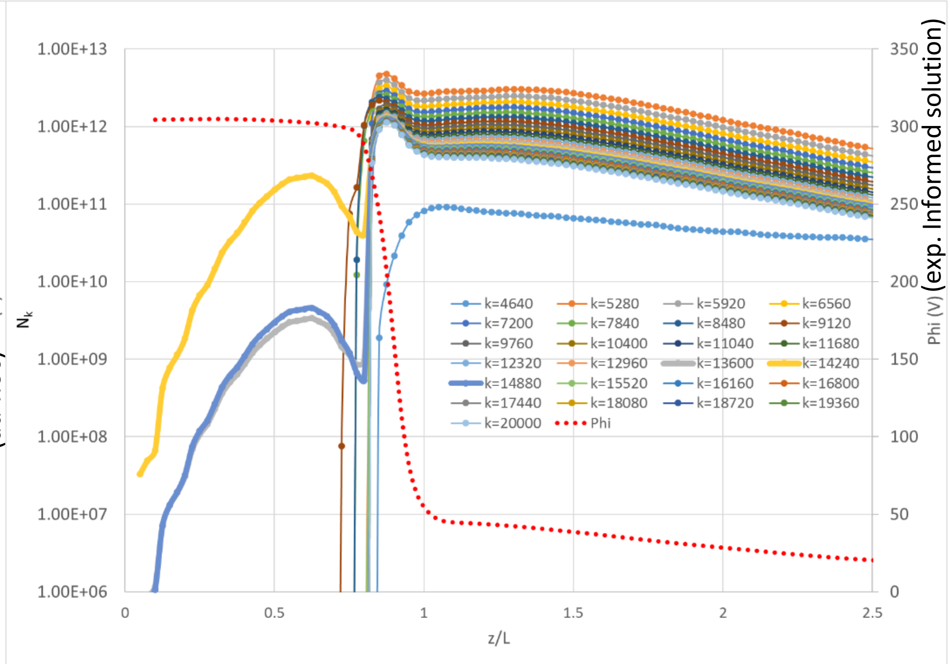

Model with **no** correction factor f_k in anomalous collision frequency

The effect of the correction factor is noticeable when computing the anomalous collision frequency

- First check for self-consistent model: **experimentally informed solution** as background for computing anomalous collision frequency based on the previous equations. **Then compare result with the experimentally informed collision frequency.**

Anomalous collision frequency decreases when ξ_k large

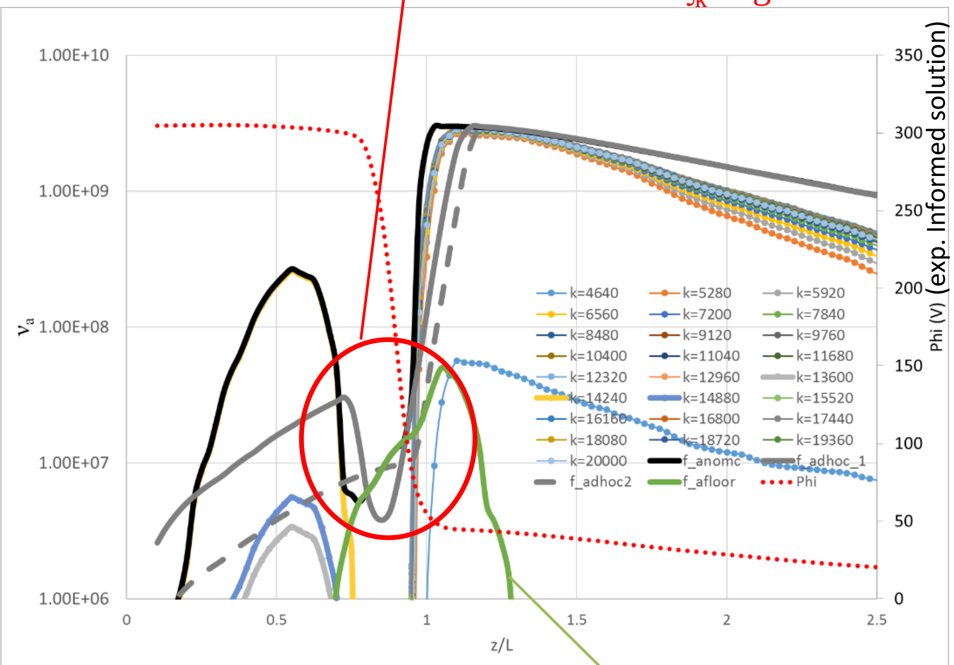

Floor of anomalous collision frequency

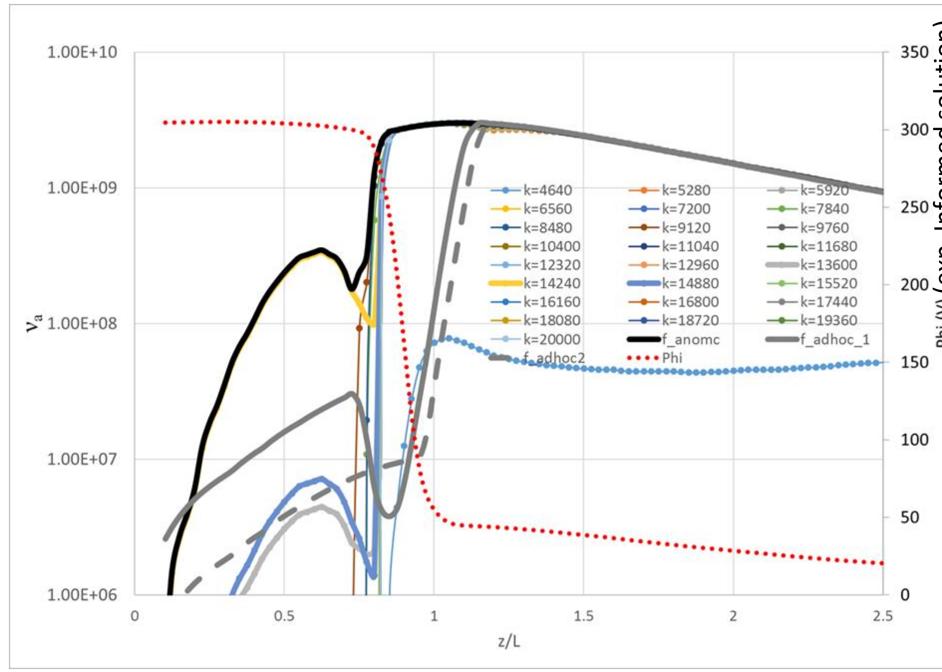

Model with correction factor f_k in anomalous collision frequency

Model with **no** correction factor f_k in anomalous collision frequency

Self-consistent simulation predicts location of acceleration region

- As the comparison between the self-consistent and the experimentally informed profiles of the anomalous collision frequency (when using the experimentally informed solution as background) has been greatly improved, we proceed to run a fully self-consistent simulation.

$$\frac{\partial \xi_k}{\partial t} - K_1 \nabla^2 \xi_k = \frac{\phi_{drift}}{\phi_k} \qquad \nu_{an} = \left(\frac{\pi}{2}\right)^{1/2} \sum_k f_k \frac{q k^2 N_k}{n_e \sqrt{m_e m_i}\left(1+k^2\lambda_{De}^2\right)^{3/2}} \exp\left(-\left(\frac{\hat{k}\cdot \mathbf{u}_{ei} - c_s \big/ \left(1+k^2\lambda_{De}^2\right)^{1/2}}{v_{te}}\right)^2\right) \qquad f_k = \exp\left(-K_2 \xi_k\right)$$

K_1 = fixed

K_2 = iterative procedure to achieve discharge current of 20 A

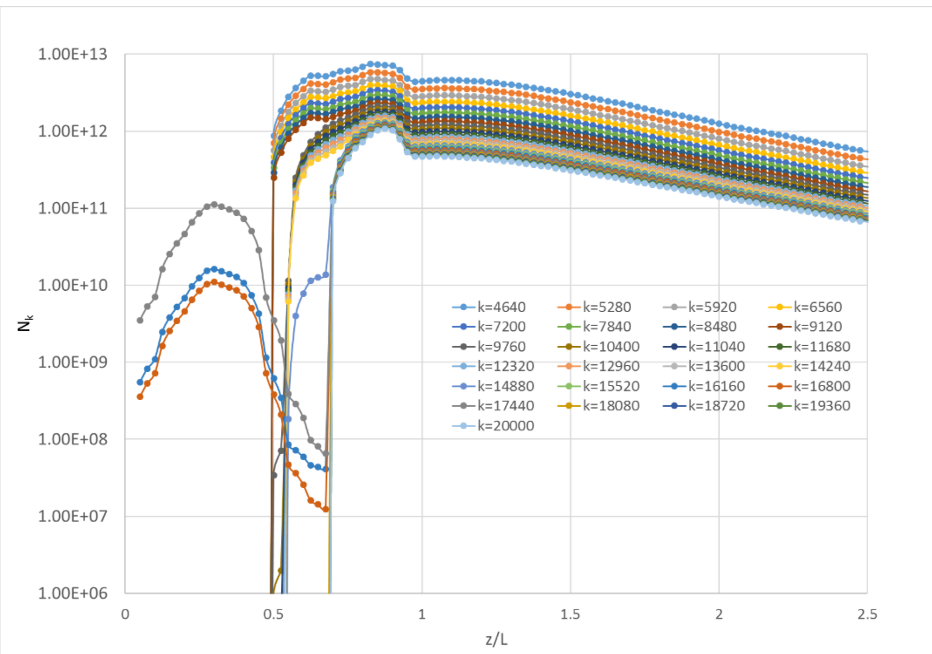

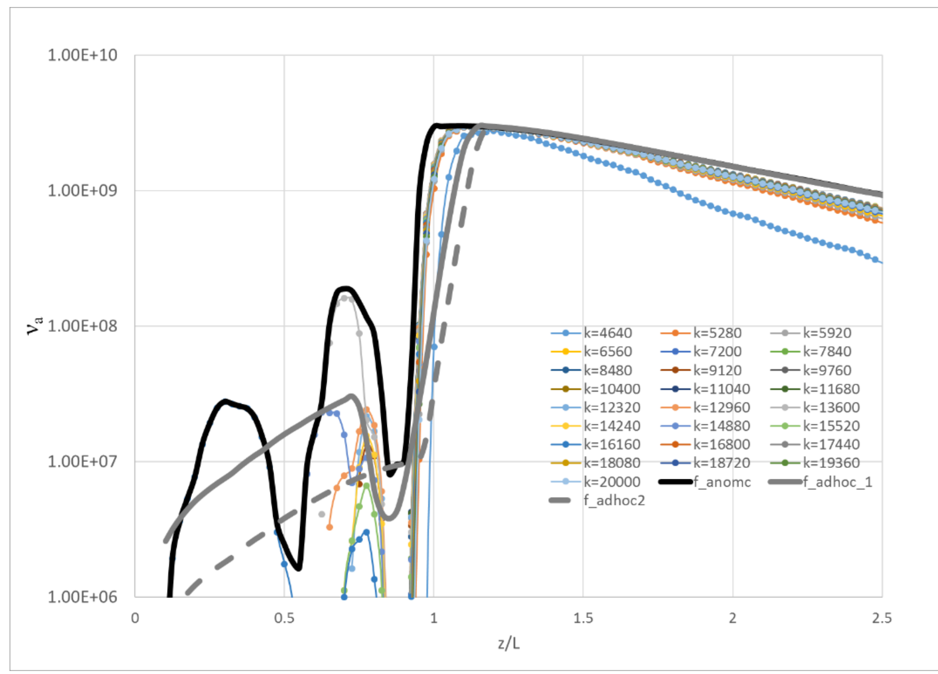

Plasma potential and anomalous collision frequency comparison

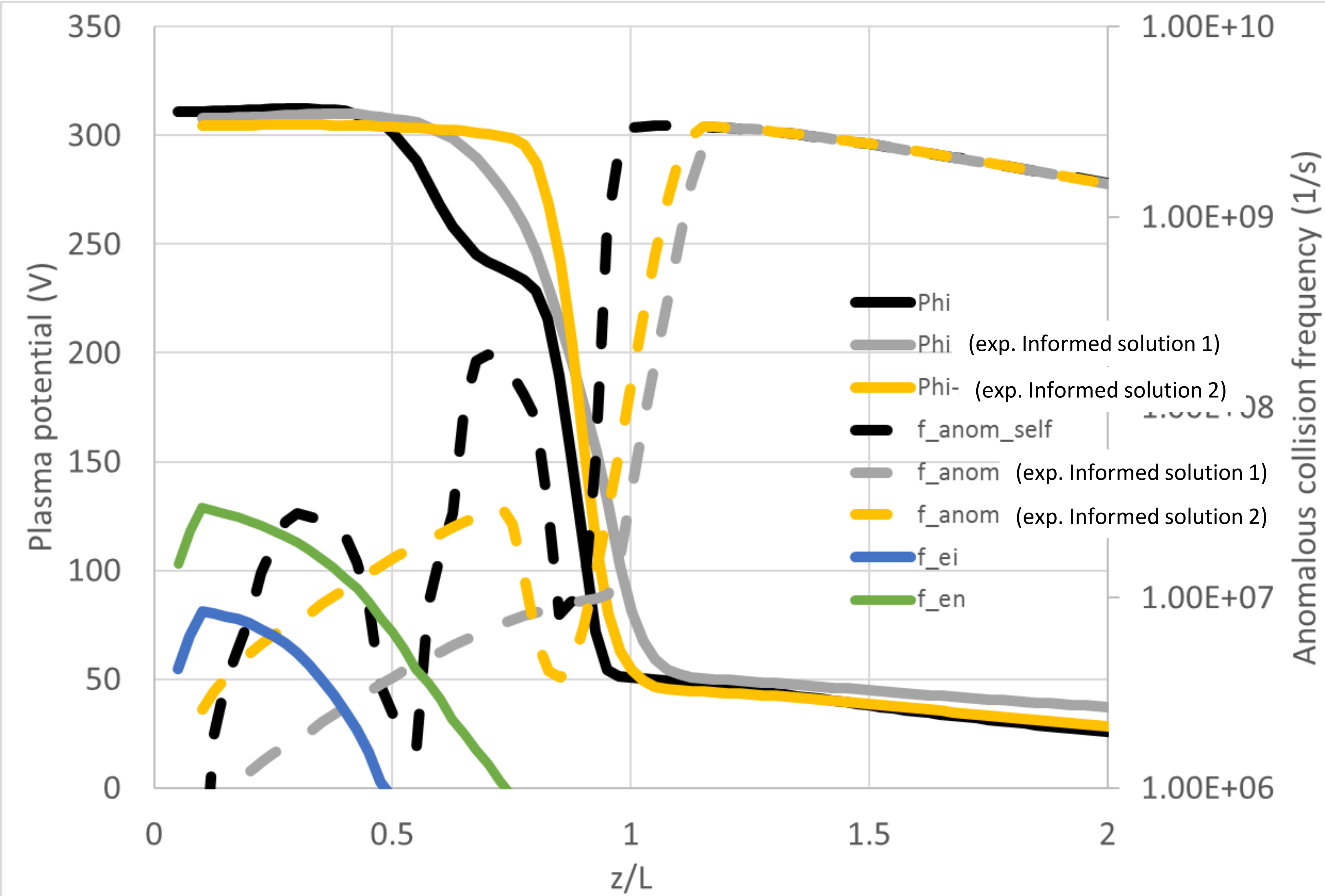

Electron temperature and anomalous collision frequency comparison

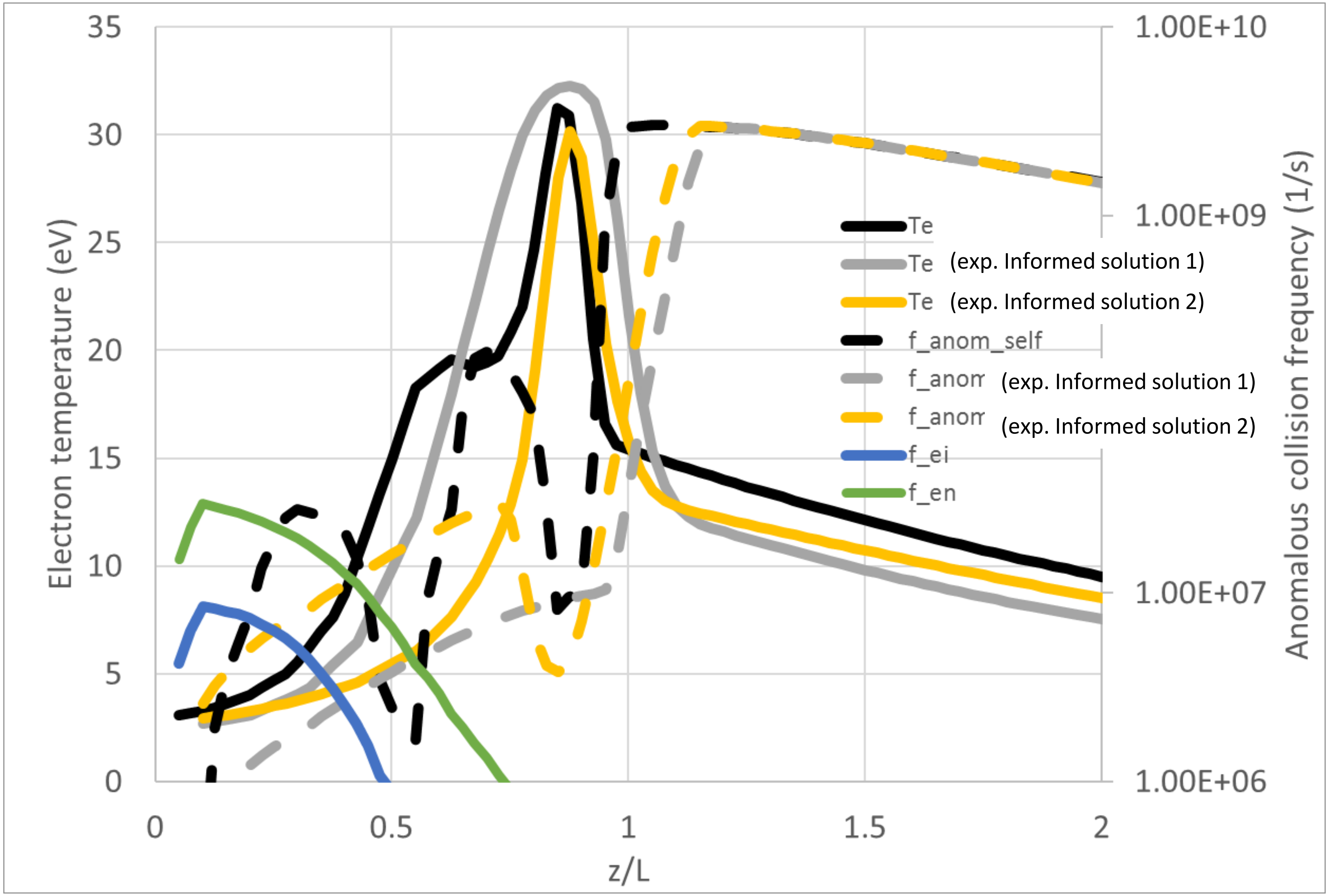

2-D Plasma potential comparison

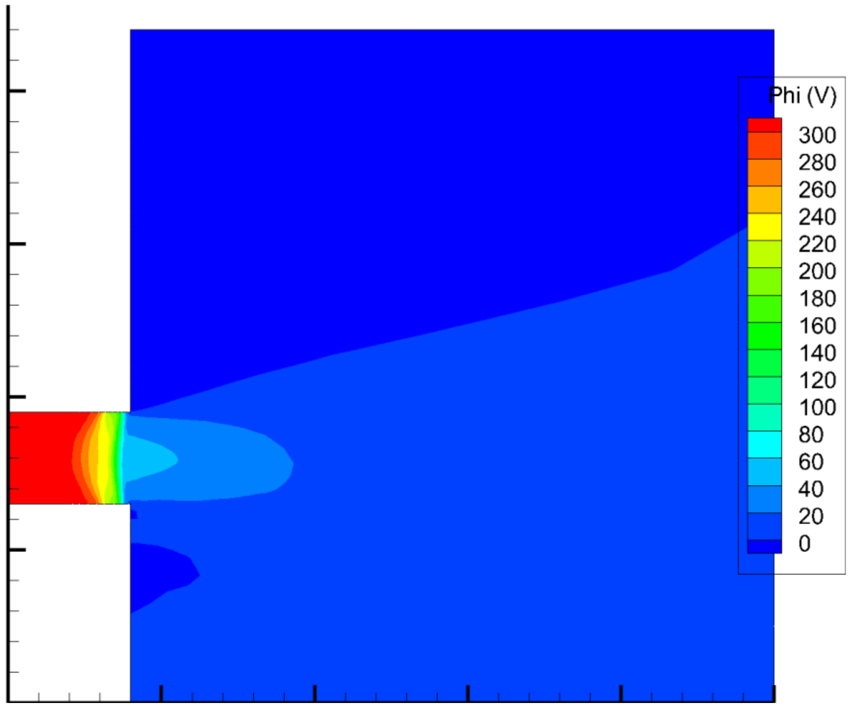

Self-consistent simulation

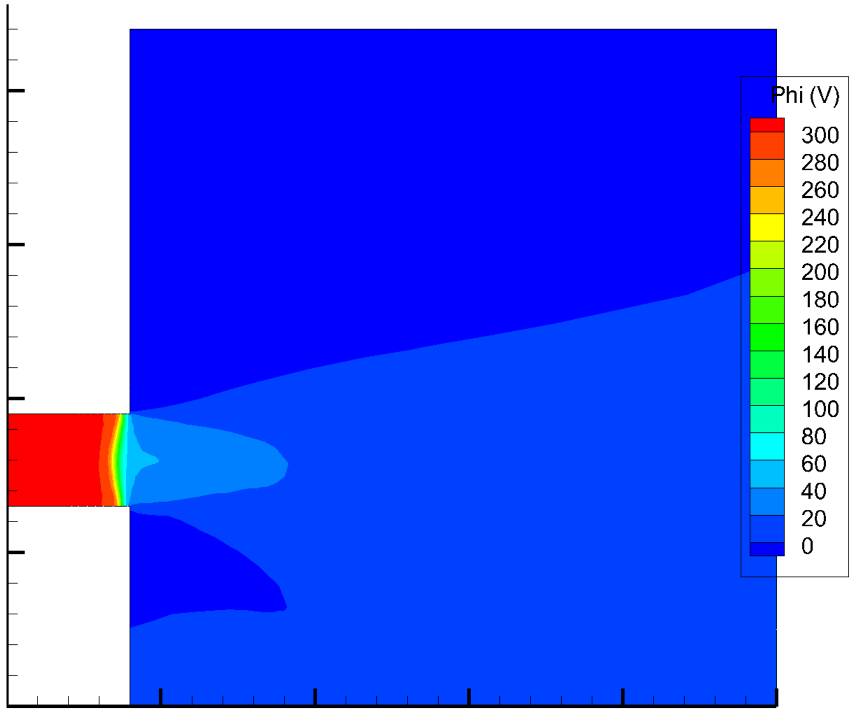

Simulation based on experimentally informed anomalous collision frequency

2-D wave energy density and anomalous collision frequency

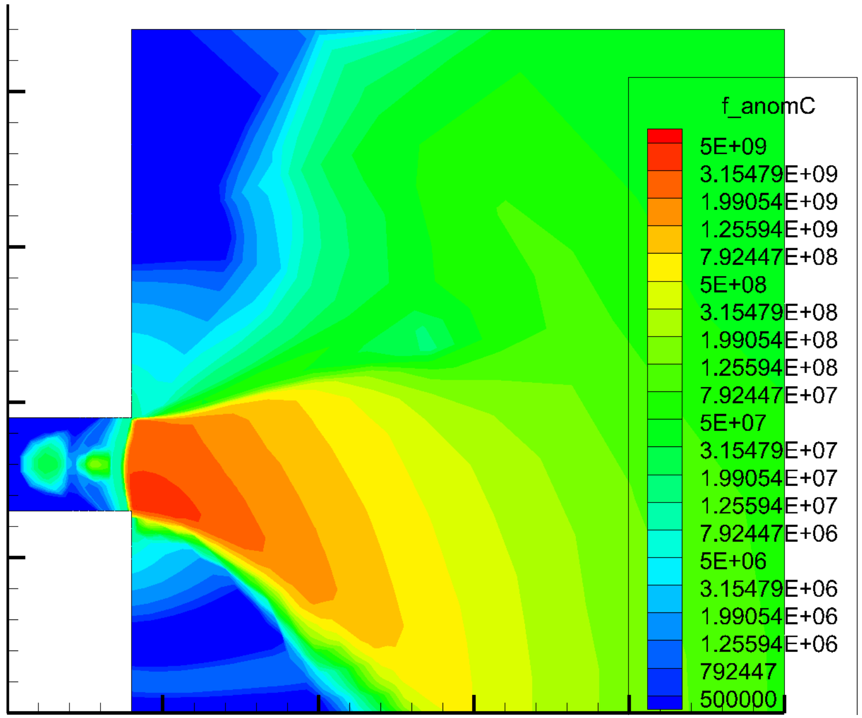

Anomalous collision frequency

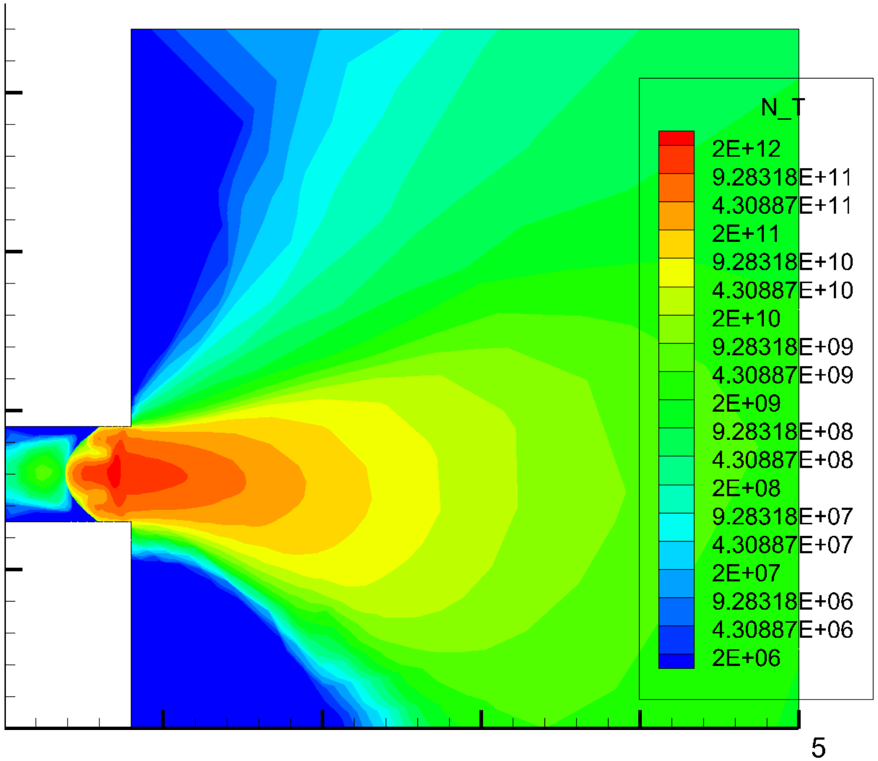

Total wave action

Concluding Remarks

- By examination of the experimentally informed solution, we came to the conclusion that its associated anomalous collision frequency solution was not achievable when employing a wave energy equation with growth terms dictated by linear theory of ion acoustic waves, assuming cold Maxwellian ions. Warm ions could however have a significant effect.
- The major difficulty was to reconcile the fact that the anomalous collision frequency is minimum when the electron drift is maximum (and thus the growth rate of the instability is maximum).
- We attempted to decrease the growth rate in the acceleration region by separating the contributions of multiple wave-lengths to the wave action and also by including the additional anomalous ion heating. This approach was proven unsuccessful as the growth rate in the acceleration region is typically much larger than Landau damping.
- We finally focused on the hypothesis that the electron transport may not be affected by ion-acoustic waves in the acceleration region. We proposed to use a simple comparison between the drift energy of the electrons and the energy of the waves to quantify this phenomenon. We also limited the floor value of the anomalous collision frequency so the Mach number for electrons never exceeds 1.
- The anomalous collision frequency solution obtained with this model exhibited good agreement with the experimentally informed profile when using the experimentally informed plasma solution as background. Full self-consistent simulations also predicted correctly the location of the acceleration region.
- Based on the promising results of this investigation, we believe that the path forward involves a detailed study of the physics of the acceleration region and whether the electron-wave interactions need to be quantified with non-linear models instead of being derived from quasi-linear theory.

BACKUP

Preamble: IAT Predicted to Drive Electron Transport in the Hollow Cathode Near-Plume as Early as 2004 [1-3].

- Classical electron collisions in 2-D hollow cathode simulations not sufficient to explain plasma measurements (just like in Hall thruster codes)
- Current-driven ion acoustic waves proposed as the “anomalous” mechanism in these devices [1-3]
  - Electron drift speed > ion sound speed generates ion acoustic turbulence (IAT)
  - IAT scatters electrons

OrCa2D Global Simulations of the NSTAR DHC [3]

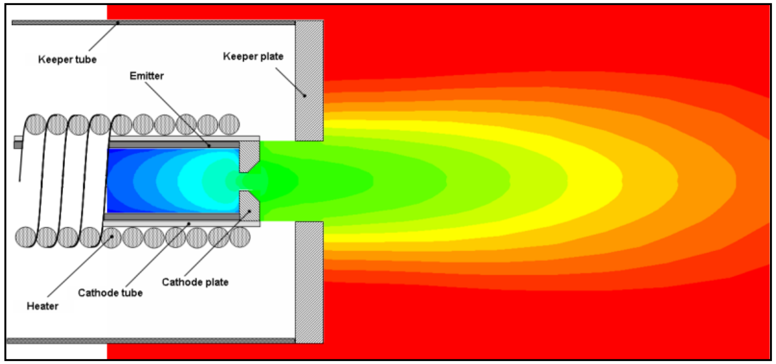

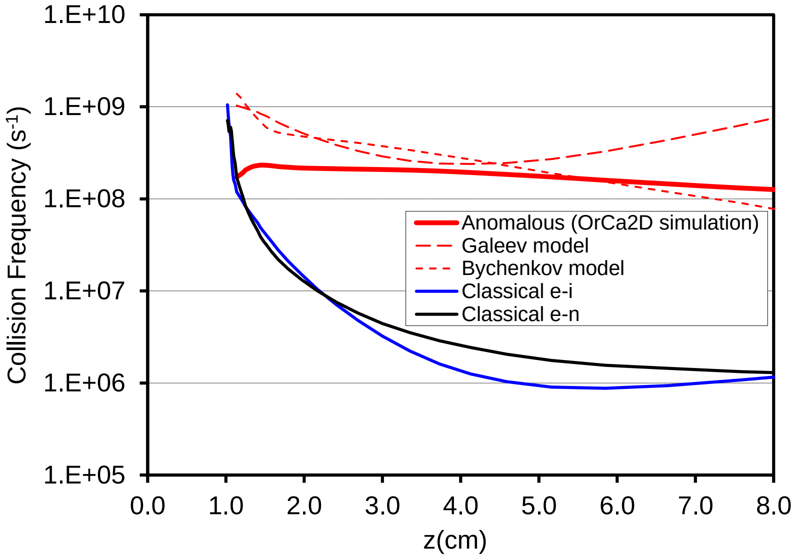

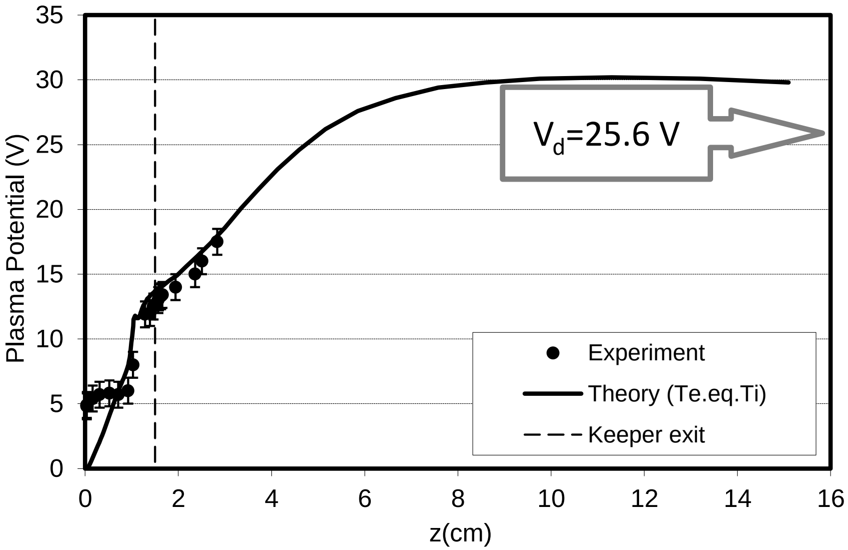

[1] Mikellides, I. G., Katz, I., Goebel, D. M., and Polk, J. E., "Hollow Cathode Theory and Experiment, II. A Two-Dimensional Theoretical Model of the Emitter Region," *J. Appl. Phys.*, Vol. 98, No. 11, 2005, pp. 113303 (1-14).

[2] Mikellides, I. G., Katz, I., Goebel, D. M., and Jameson, K. K., "Evidence of Non-classical Plasma Transport in Hollow Cathodes for Electric Propulsion," *J. Appl. Physics*, Vol. 101, No. 6, 2007, pp. 063301 (1-11).

[3] Mikellides, I. G., Katz, I., Goebel, D. M., Jameson, K. K., and Polk, J. E., “Wear mechanisms in electron sources for ion propulsion, 2: Discharge hollow cathode,” *J. Prop Power*, 24 (2008) 866-879.

IAT Confirmed by Measurement to Exist and Drive Electron Transport in the Hollow Cathode Near-Plume [1,2]

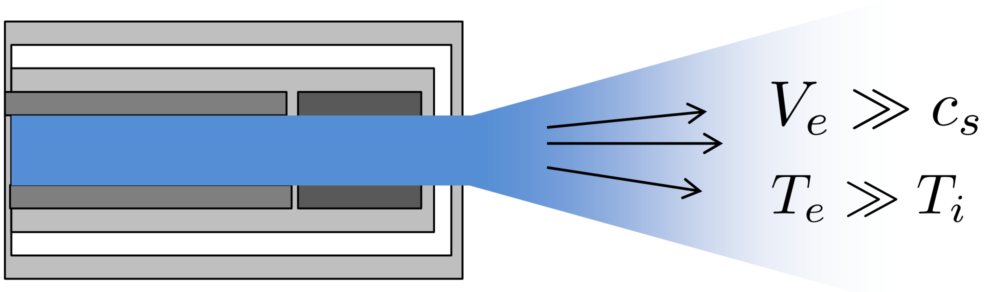

Electron drift exceeds ion sound speed

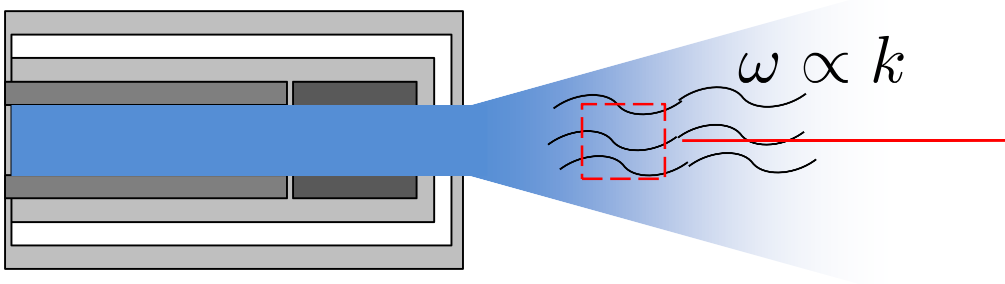

Ion acoustic turbulence grows at expense of electron drift

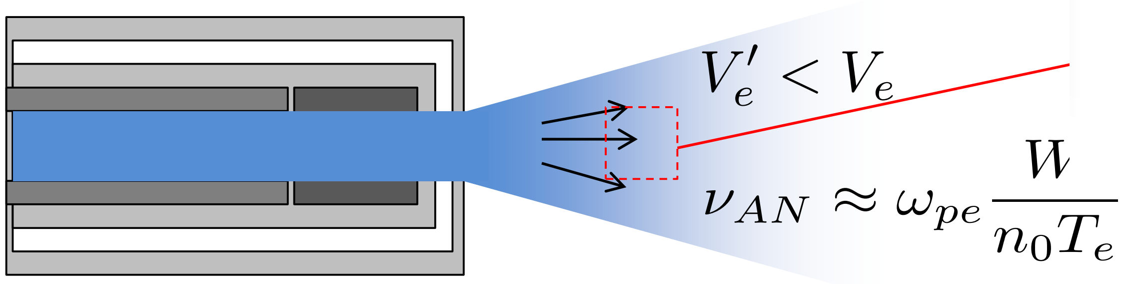

Growth of IAT slows electrons

Wave dispersion diagnostics confirm long-suspected presence of IAT

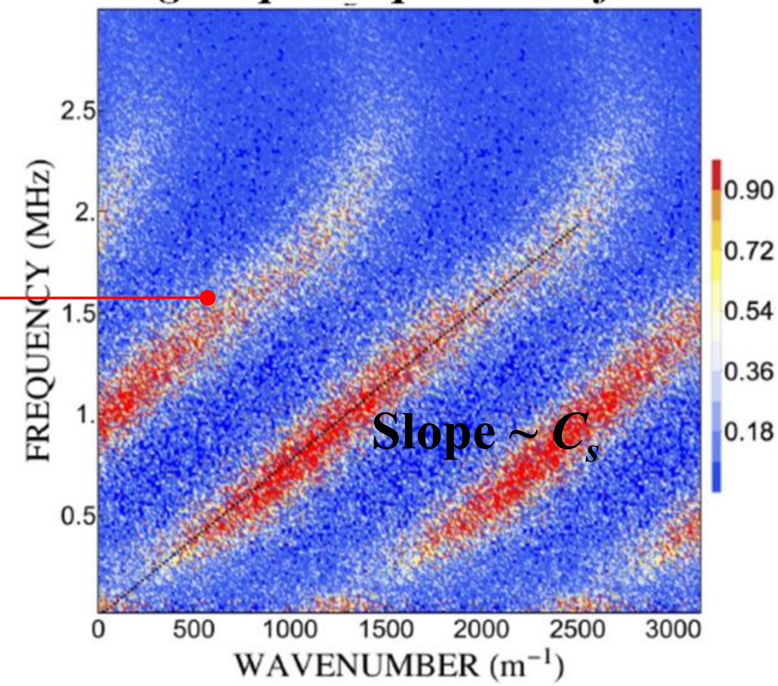

[1] Jorns, B. A., Mikellides, I. G., and Goebel, D. M., "Ion Acoustic Turbulence in a 100-A LaB6 Hollow Cathode," *Physical Review E*, Vol. 90, 2014, pp. 063106 (1-10).

[2] Jorns, B. A., Mikellides, I. G., and Goebel, D. M., “Investigation of a Energetic Ions in a 100-A Hollow Cathode,” AIAA Paper No. 14-3826, 50th Joint Propulsion Conference, Cleveland, OH, July 2014

Lampe et al. (1972) Showed Electron Cyclotron Waves in a Plasma with Crossed **E,B** Transition to Ion Acoustic Waves [1]

- When electron drift is high enough or when B→0 cyclotron harmonics disappear and the unstable spectrum approaches the usual 2-stream instability (continuous spectrum).
- Lampe proposes "…***B** does not create a new instability but rather quantizes the unstable spectrum into discrete bands*."

Linear theory

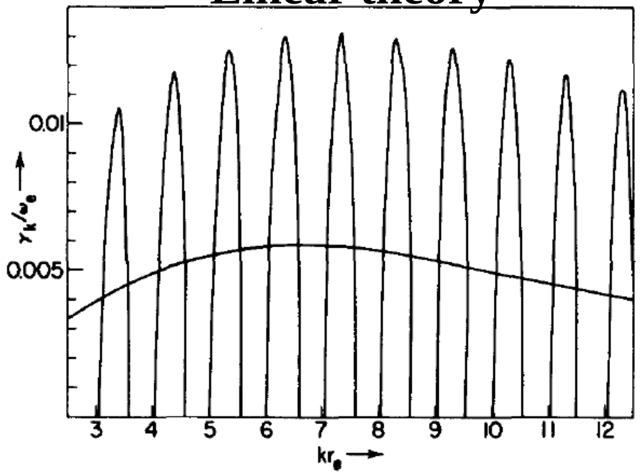

FIG. 1. Growth rate vs wavenumber for a hydrogen plasma with $v_d/v_e=1$, $T_i/T_e=0$ for the cases $\Omega_e/\omega_e=0.1$, $\Omega_e=0$ (smooth curve).

PIC simulations

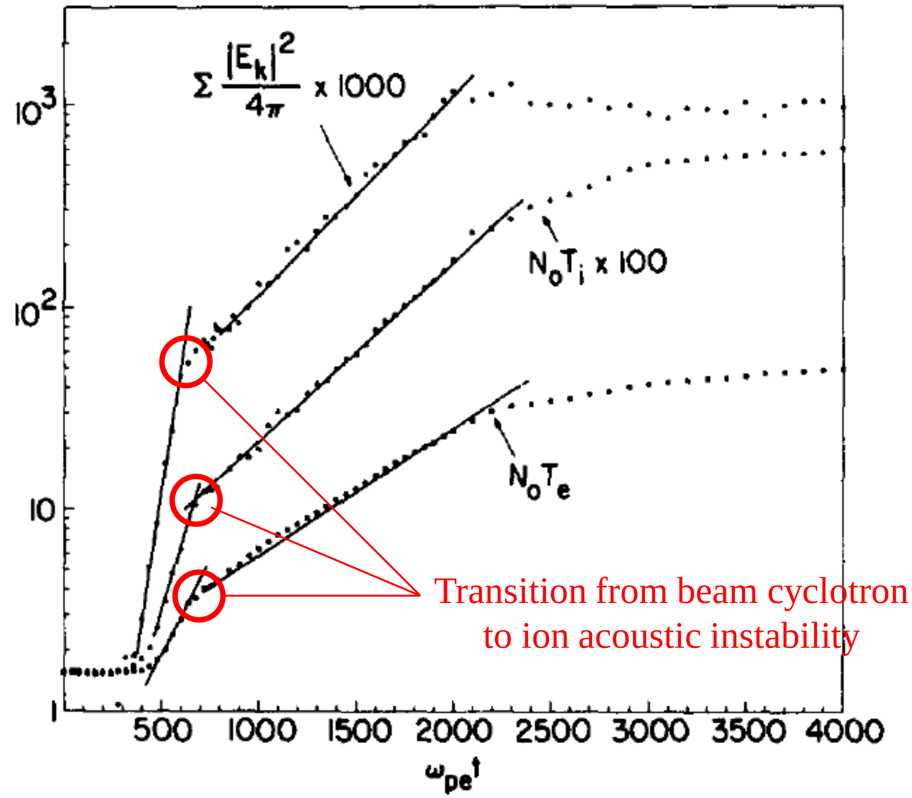

FIG. 5. Plots of electrostatic $(\Sigma|E_k|^2/4\pi)$, electron thermal (N_0T_e), and ion thermal $(\frac{1}{2}N_0T_i)$ energy densities, for run 3. Energy units are arbitrary. The solid lines are drawn to emphasize the exponential behavior during the quasilinear stages. Note that electron heating is isotropic in two dimensions because of the magnetic field, while ion heating is one-dimensional.

[1] M. Lampe, W. M. Manheimer, J. B. McBride, J. H. Orens, K. Papadopoulos, R. Shanny, and R. N. Sudan, "Theory and Simulation of the Beam Cyclotron Instability", Physics of Fluids 15, 662 (1972)

Example of ξ_k (for k=11680 m^{-1})